ATL-DAQ-99-014
18 Oct 1999

Detector and Read-Out Specification, and Buffer -RoI Relations, for Level-2 Studies

Abstract

This note, an update to DAQ Note 62, is intended to summarise the present state of knowledge of the modularity, η–ϕ ranges, channel count and segmentation of each detector into the RODs and hence ROBs. The data format,where known, arising from each detector is also summarised, as well as information on occupancy and data volume per ROB at high and low luminosity.

Authors : P.Clarke, S.Falciano, P.Le Du, J.B.Lane, M.Abolins, C Schwick, F.J.Wickens

NoteNumber : ATL-COM-DAQ-99-017
Version : 1.00
Date : October 1999
Reference :

1 Definitions

Certain acronyms are used in this document which might have different interpretations by different readers. To avoid ambiguity they are defined here as used in this document:

ROD: A read out driver, part of the detector front-end, where data from a detector is prepared and sent to the ATLAS central DAQ system.

ROB: A read out buffer having a 1:1 correspondence to a ROD.

MUR: The "Minimum Unit of Readout within a detector". This means the minimum unit which is read out as a single collective block of data, and which therefore forms the smallest unit of flexibility as regards grouping of channels into RODs.

FEX: A feature extractor, the processing units where feature extraction is performed on the data from a single detector within an RoI.

2 Transition Radiation Tracker (TRT)

2.1 Geometry

The geometry is unchanged since *[1]*. Further details have been taken from *[2]*.

2.1.1 Barrel

The barrel consists of three concentric cylindrical rings. Each ring is formed from 32 independent identical mechanical modules. The modules are not projective and have a different shape from ring to ring. The familiar zig-zag shape formed from concentric modules is shown in figure 1.

Each mechanical module extends to +- 0.8m in z. Each module contains straws running parallel to the beam axis. Each straw is divided into two at the centre (z=0), and each half is read out separately. This means that the TRT is effectively divided into two independent barrel halves in the ranges -0.8 to 0m and 0 to 0.8m respectively.

The geometry, module count and channel count is given in table1 below. The TRT barrel covers the range $|\eta| < 0.7$

2.1.2 Endcap Wheels

Each endcap consists of 18 wheels. The nearest wheel is at z=0.83m and the furthest is at z=3.36m. The range of η covered is approximately 0.7 to 2.5.

Each wheel contains several layers of straws spaced along z, with the straws in each layer running out radially from the centre. There are three different types of wheel:

Layer	Approx radius (cm)	z range (mm)	#mechanical modules	# channels /module	Channels
inner	*56-69*	*+- 800*	*32*	*329 x 2*	*10528 x 2*
middle	*69-85*	*+-800*	*32*	*520 x 2*	*16640 x 2*
outer	*85-107*	*+-800*	*32*	*793 x 2*	*25376 x 2*
Total				**1642 x 2**	***52544 x 2***

Table 1: Geometry, module and channel count of TRT Barrel. The x2 factor is shown to make the division of each straw at z=0 explicit.

Each of wheels 1-6 extends from 640 - 1030 mm in radius and contains 12288 straws.

Each of wheels 7-14 extends from 640 - 1030 mm in radius and contains 6144 straws (essentially identical to 1-6 but with fewer straw layers).

Each of wheels 15-18 contains extends from 480 - 1030 mm in radius and contains 9216 straws.

In total there are 159744 straws in each endcap.

The arrangement is illustrated in figure 2 .

2.2 Readout segmentation

The barrel is divided logically into 32 projective readout wedges in phi, per side (therefore 64 readout wedges in all). In each such readout wedge channels from all three rings are grouped together to be read out into one ROD. These logical wedges do not follow the mechanical segmentation, but are instead formed by grouping channels from adjacent modules in all three rings to form truly projective sets. Thus the mechanical segmentation is irrelevant to the subsequent readout of data from the RODs. This is illustrated in figure 1. **There are therefore 64 ROBs associated with the entire barrel.**

Each endcap is divided logically into 96 sectors. In each such sector channels from all 18 wheels are grouped together to be read out into one ROD. This is illustrated in figure 2. **There are therefore 96 RODs per endcap.**

The segmentation, η–ϕ range and ROD count are shown in table 2 below.

TRT Readout segmentation into a single ROD	$\Delta\phi$	η	channels/ ROD	#RODs
One barrel wedge	*0.2*	*0.0-0.7*	*1642*	***64***
One endcap wedge	*0.07*	*0.7-2.5*	*1664*	***96 x 2***

Table 2: TRT readout segmentation into RODs.

2.3 Occupancy

In the TRT, occupancy is defined as the fraction of straws that are hit per bunch crossing. In calculating data volumes, allowance must be made for the fact that data from three consecutive bunch crossings are considered. The TRT occupancy at high luminosity is high. Figures presented in *[2]* vol.1-p97 indicate 10-40% in the barrel and about 20% in the endcap. For the purposes of this document an average of 20% is assumed.

The TRT occupancy at low luminosity is expected to be up to a factor of 10 lower. For this document we use a conservative figure of 4%.

2.4 Data into ROD

The data into the ROD contains, for each straw, information corresponding to the level-1 trigger BX plus the two following BXs. For each BX there is 1 bit to indicate the state of the high threshold discriminator, and 8 bits to indicate the state of the low threshold discriminator each 3 ns (actually 25/8 = 3.125ns). Thus there are 27 bits per channel. This information is transmitted for each of the 1642 /1662 channels.

The data volume into each ROD is therefore about **50 kbits/event** (1642 x 27 bits + headers + byte alignment).

2.5 Data from ROD to ROB

The data is compressed in the ROD before transmission to the ROB *[2]*vol.2-p830, *[3]*.

The low threshold bits are inspected in a 12ns window set at approximately 42ns from the level-1 accept BX (this means that the window is in the 2nd BX period). If any bit is set then the straw is declared as 'VALID'. In this case leading edges in the first two BXs are sought (i.e. 0->1 transitions in low threshold bits) and depending upon the result the following is transmitted:

If 0 leadingedges:	<01><1><L&H><T>	(5 bits)
If 1 leading edge:	<10><tttt><H><T>	(8 bits)
If 2 leading edges:	<11><ttt><ttt><H><T>	(10 bits)

If the straw is NOT VALID then:

If no threshold bits set: <00>	(2 bits)
If any threshold bits set: <01><0><L&H>	(4 bits)

where:
<tttt> or <ttt> are a 4-bit or 3-bit encoding of the hit time respectively,
<H> is a one bit OR of all of the high threshold bits
<L> is a one bit OR of all of the low threshold bits
<L&H> is a one bit encoding of all the low and high threshold bits

<T> is one bit to indicate that a trailing edge ocurred in the third BX.

Clearly this scheme leads to a large range of possible data sizes. The following model is used to estimate the data volume with sufficient accuracy for this document. At 20% occupancy then out of the 1640 channels per ROD there will be up to 330 per event with valid hit information which we take to require 8 bits on average. All information is assumed to be 4-bit aligned. This results in approximately **8 kbits/event** transmitted to each ROB (330x8 + 1310x4 + headers) at high luminosity.

At low luminosity a 4% occupancy reduces this to around **6 kbits/event**.

Information on the ROD-ROB data rate as a function of luminosity is given in section 13.4.4.2 of the Inner Detector TDR, Volume 2..

2.6 Data from ROB to FEX

At this point it is possible to either send some bits for each straw or a zero suppressed list with addresses. Due to the high occupancy it is not obvious which results in the lowest data volume, especially at high luminosity. The breakeven point is between 20-30% occupancy but depends upon byte alignment policy. To complicate the issue it is also not known definitively whether the time information is required by the FEX algorithm.

Given that there are a large number of hit type possibilities enumerated in the previous section, the minimum processing could be to make a simple hit/no hit decision for the purposes of the trigger (according to the number and position of edges etc). Following this a suitable number of bits per hit straw could be 1 high threshold bit + 4 drift time bits, i.e.:

for each no-hit straw:	<0>	(1 bit)
for each hit straw:	<1><H><tttt>	(6 bits)

However if 4-bit alignment is required the total volume would not be reduced.

If instead a zero suppressed list were send then a suitable format would be:

<aaaaaaaaaaa><H><tttt> (16 bits)

where <aaaaaaaaaaa> is an 11 bit straw address. This would result in a data volume of 5.5 kbit/ROB/event (330x16 + header).

We therefore conclude that pre-processing in the ROB could reduce the data volume by **a factor of 0.7** at high luminosity.

At present it looks unlikely that any other processing in the ROB would be useful. Specifically no part of the hough transform feature extraction *[4]* can easily be devolved to the ROB without actually causing more data to be transferred rather than less.

Figure 1: TRT Barrel Readout Segmentation

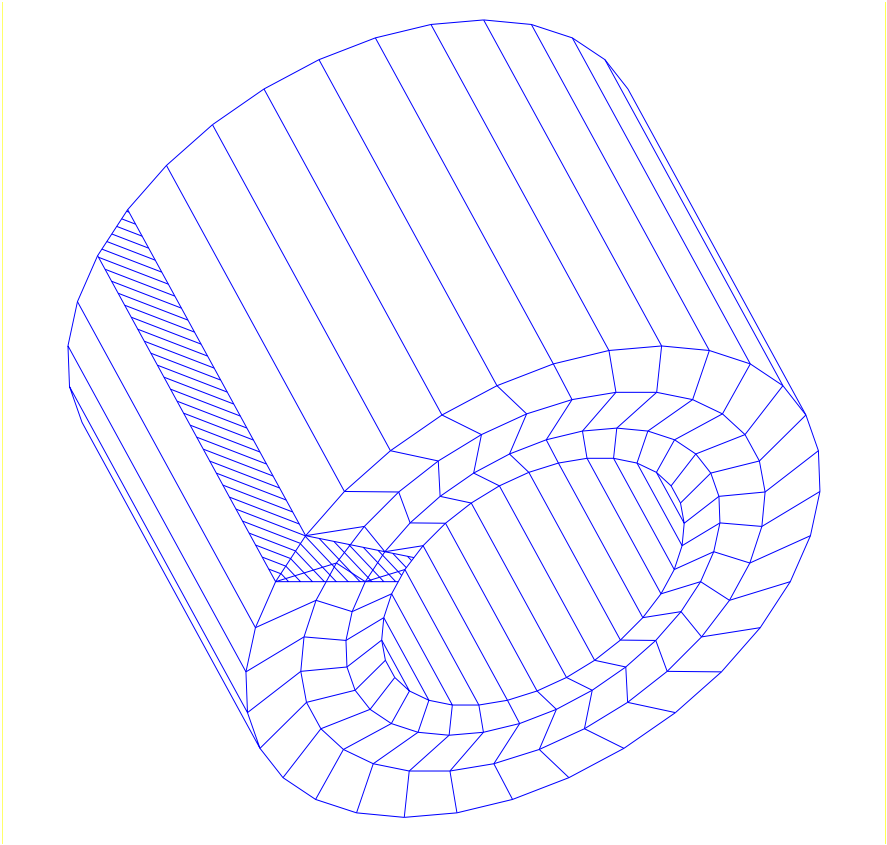

Figure 2: TRT Endcal Readout Segmentation

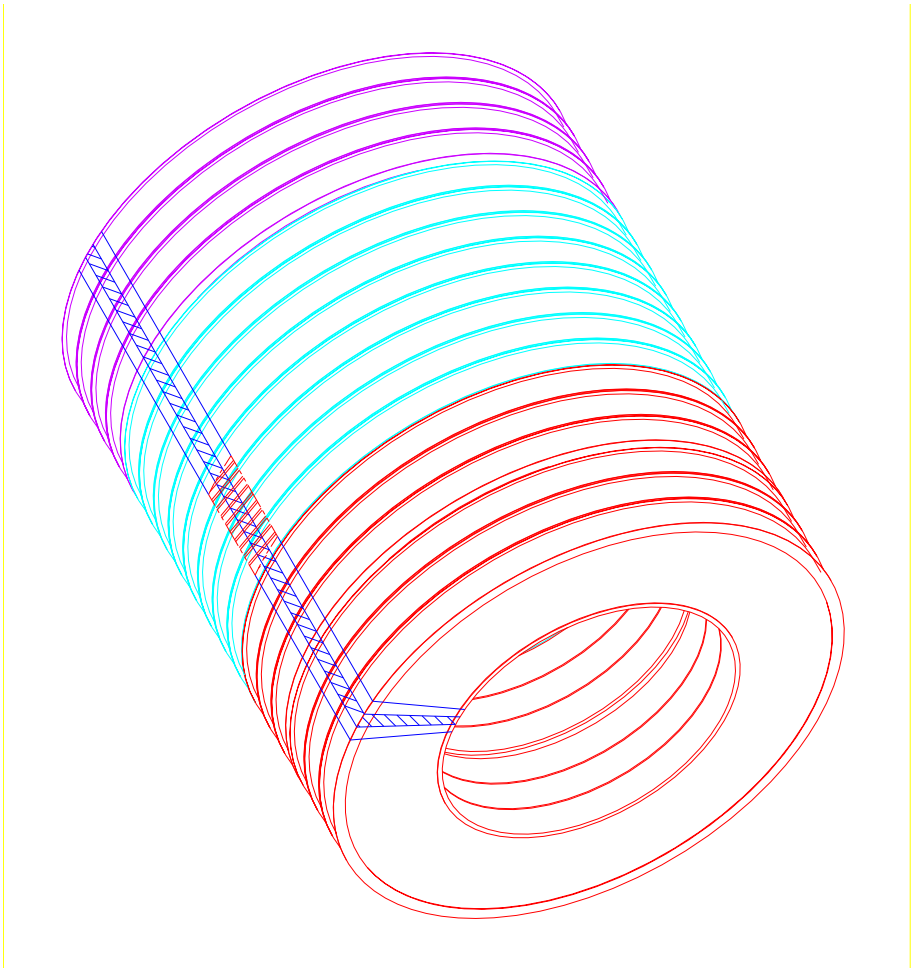

3 The Silicon Strip Semiconductor Tracker (SCT)

3.1 Modules

The basic sub-unit of the SCT is a module. There is a single module design for the barrel, and three designs for the endcap wheels to accommodate three possible radial locations. All modules are functionally similar.

A barrel module consists of a set of silicon strip detectors joined lengthways and glued together to effectively form a double sided structure of width 64 mm and strip length 128mm. On one side a small stereo angle of 40 mrad is introduced. There are 768 strips per side, 1536 per module in total.

The endcap modules are formed by joining and glueing silicon strip detectors together to form double sided sectors of a ring. The strips run in the radial direction (i.e. they have increasing pitch so that they fan out to follow the radial coordinate). On one side a small stereo angle of 40 mrad is introduced. There are 768 strips per side, 1536 per module in total.

3.2 Geometry

Geometry details have been taken from the TDR *[2]*. The geometry is unchanged since *[1]*.

3.2.1 Barrel

The barrel is constructed as four concentric cylinders (layers). Each layer is constructed from ladders containing 12 modules along the axial (z) direction. Modules are oriented with their strips running in the z direction such that co-ordinate information is provided in the r-ϕ plane. The total number of modules and channels in each layer are given in table 3 below. In total there are 2112 modules in the entire barrel and approximately 3.2 x 10^6 channels. The barrel detector covers the eta range +- 1.4.

Layer	Radius (mm)	z range (mm)	#ladders (in ϕ)	#modules on ladder	#modules in layer	Channels (1536/mod.)
1	*300*	*+- 747*	*32*	*12*	*384*	*589824*
2	*373*	*+-747*	*40*	*12*	*480*	*737280*
3	*447*	*+-747*	*48*	*12*	*576*	*884736*
4	*520*	*+-747*	*56*	*12*	*672*	*1032192*
Total					**2112**	***3.2 x 10^6***

Table 3: SCT Barrel: Geometry, module and channel count.

The barrel arrangement is shown in figure 3.

3.2.2 The endcap wheels

There are 9 wheels in each endcap region, spaced along the z direction. Each wheel consists of up to three rings of modules depending upon the position. All strips run radially outward so that phi information is provided by each wheel. The details of position, module and channel count are given in table 4 . In total there are 988 modules/endcap with approximately 1.5 x 10^6 channels/endcap. The endcap covers the eta range 1.4 - 2.5.

Wheel	r range (mm)	z (mm)	#modules in. / mid./ out.	Channels (1536/mod.)
1	*259-560*	*835*	*40/40/52*	*202752*
2	*336-560*	*925*	*-/40/52*	*141312*
3	*259-560*	*1072*	*40/40/52*	*202752*
4	*259-560*	*1260*	*40/40/52*	*202752*
5	*259-560*	*1460*	*40/40/52*	*202752*
6	*259-560*	*1695*	*40/40/52*	*202752*
7	*336-560*	*2135*	*-/40/52*	*141312*
8	*401-560*	*2528*	*-/40/52*	*141312*
9	*440-560*	*2788*	*-/-/52*	*79872*
Total (x 2 ends)			**988 (1976)**	*1.52 x 10^6 (3.04 x 10^6)*

Table 4: SCT Endcap: Geometry, module and channel count.

The endcap arrangement is shown in figure 4.

3.3 Readout segmentation

3.3.1 Barrel

Each module is read out independently by two fibres (one for normal and one for stereo layer - although the electronics allows both to be read via any one fibre in the event of failure). There is also a single control fibre going to each module.

Each ladder (i.e. 12 modules running in z) is read out in two halves, 6 modules going to each end. Each “half ladder” is connected to one harness which contains a 12-fibre ribbon (2 fibres per module) for data and a 6-fibre ribbon for the control signals. These ribbons end in a 12-way MT12 and a 6-way MT6 optical connector respectively. Therefore one might think that the basic unit of readout would be this “half ladder”. However, for reasons of connector economy at the ROD, the control signals are fed down in such a way that one 12-way ribbon is split into 2x6 to feed two adjacent (in ϕ) half ladders within a layer. Therefore the minimum unit of readout (MUR) into a ROD is two adjacent half ladders.

It is planned to be able to feed up to 48 modules into one ROD [1], in other words 8 “half ladders”. This corresponds to approximately 74,000 channels.

The grouping of MURs into RODs is not yet fixed. This is the subject of a detailed study *[5]* to optimise the grouping from the point of view of the trigger ROI requests. Possible groupings that can be imagined are:

Connect adjacent sets in each layer. In this way it would be guaranteed that four RODs are required for each ROI as this is the only way to obtain all four layers. It may however be that sometimes more than four ROBs would be required. This is simple but the large $\eta-\phi$ range covered would lead to high ROB request rates. Common sense would suggest that this would be a bad grouping.

Connect some form of projective geometry by combining sets from each of the four layers into one ROD. This can only be done approximately since there are a different number in each layer, and it would be necessary to make up patterns which can be repeated with some symmetry. There is no completely obvious ‘symmetric’ looking grouping.

Previous work has been done to optimise the mapping using a simulated annealing method to minimise the number of ROBs required per ROI. Details can be found at *[6]* which are too complex to repeat here, but these are no longer applicable as they assumed flexibility at the module level.

For the purposes of this document we assume that MURs from all four layers will be grouped to form projective wedges with approximately equal ϕ segmentation. The barrel is therefore divided into 22 ϕ segments per half barrel (176 half ladders divided into sets of 8).

The grouping into RODs is summarised in table 5 below. There are 44 ROBs for the entire SCT barrel.

3.3.2 Endcap Wheels

Since there is no natural mechanical grouping of endcap wheel modules the following assumptions are made (having discussed the matter informally with members of the endcap group):

Sets of up to 6 modules within a ring will be grouped together to share one 12-way data ribbon and one 6-way control ribbon exactly as for the barrel. This will form the minimum unit of readout (i.e. for the present we do not assume the two adjacent half-ladder constraint).

The exact patterns chosen will repeat in each quadrant of a wheel due to the symmetry of service routing.

Up to 48 modules, equivalent to 8 MURs, will be concentrated into a single ROD.

---

1. If technical complexities concerned with the clock and control optical links, or bandwidth limitations of the readout link to the ROB, cannot be overcome then the number might be reduced to 36.

An example of a suitable ‘common sense’ grouping [1] within a wheel is shown below:

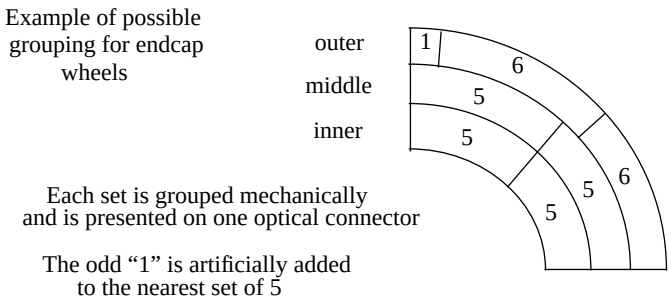

The mapping into RODs is also under study *[5]*. We may however also presume that it is sensible to combine successive wheels into an approximate projective wedge geometry. Given the non-overlapping geometry of the wheels, it is not necessary to combine all 9 wheels. Obvious possibilities are to combine a set of four and a set of five wheels, or three sets of three wheels.

For the purposes of this document we assume that wheels are grouped such that one ROD receives the connectors from one ‘octant’ (i.e. a 6+5+5 or 6+1+5+5 set) from each of 3 successive wheels. In other words the grouping divides the endcap into 8 octants in ϕ and 3 sections along the z axis.

The grouping into RODs is summarised in table 5 below. This mapping yields 24 ROBs per endcap (the minimum possible @ 48 modules per ROD is 21).

SCT Readout segmentation into a single ROD. (undecided, these are some options)	$\Delta\phi$	η	**channels/ ROD**	**#RODs**
Barrel: 8 half ladders from all 4 layers in approximate projective geometry (subject to two adjacent half-ladder MUR)	*~0.5*	*0.0-1.4*	*73728*	***44***
Endcap: 3 projective “octants” from successive wheels	*wheels1-3: 0.8* *wheels4-6: 0.8* *wheels7-9: 0.8*	*~1.2-1.9* *~1.6-2.4* *~2.0-2.5*	*≤ 73728*	***24 x 2***

Table 5: SCT readout segmentation into RODs.

1. In this scheme there would be three sets of 6 and three sets of 5, and even fewer sets of 5 in wheels with only one or two rings. Assuming the sets of 5 run in a 12-way ribbon (with one pair of fibres wasted) this leads to approximately 7% fibre wastage over the entire endcap.

3.4 Occupancy

The best estimate of occupancies are taken from *[2]* vol1-p86. Approximating these to the accuracy with which they are known we take 1% of strips for minimum bias pile-up at high luminosity and 2% inside high-p_T b-jets.

3.5 Data into ROD

The format of the data into the RODs is now almost certainly fixed *[7]*. Under normal running conditions the readout chips on the modules [1] scan the strips and only transmit information for hit strips. There are 11 bits of address information plus 3 data bits corresponding to the binary hit status of each hit strip (the triggered BX and the two BXs either side). The readout chip recognises adjacent strips ("clusters") and only sends one address followed by the 3 data bits for each strip in the cluster.

At 1% occupancy there are on average 15 hit strips per module (740 per ROD). About half of these will come as adjacent pairs, with the rest as single hits (there are rarely more than two adjacent). This yields approximately 13 kbits into each ROD/event at high luminosity. The corresponding number at low luminosity is about 2 kbits.

3.6 Data from ROD to ROB

Information taken from ROD Web pages *[8]* indicates that they will transmit the following to the ROB:

for each module: <0100><mmmmmmmmmmmm> (16 bits)

then either in non-condensed mode:

for each hit strip: <10><ddd><aaaa><ccccccc> (16 bits)

or if in condensed mode:

for each single hit strip:<11e0><0><aaaa><ccccccc> (16 bits)

for each adjacent pair: <11e0><1><aaaa><ccccccc> (16 bits)

where:

<mmmmmmmmmmmm> is the module number
<aaaa> is the 4-bit chip number within a module
<ccccccc> is the 7-bit channel number
<ddd> are the 3 data bits for BX-1, BX, BX+1
<e> is an error bit

1. There are actually 12 ABC readout chips per module, each responsible for 128 channels. This is not really important to this document.

The data volume, based upon 15 hits/module is approximately **12.5 kbits/ROB/event** ([16+15x16]x48 + headers) at high luminosity. The corresponding number at low luminosity is about **2 kbits/ROB/event.** Note that the number at high luminosity takes into account the higher occupancy inside Regions of Interest (i.e. inside jets), whereas the number for low luminosity is for the average occupancy over the whole detector (i.e. relevant for B-physics). These calculations ignores condensed mode which would reduce the volume by 20%.

3.7 Data from ROB to FEX

It will almost certainly be necessary to select the ROI data within the ROBs since the region encompassed by a single ROB is far greater than an ROI region. The data volume reduction factor is approximately *20*.

It is not necessary to use the three data bits <ddd>, therefore a simple selection of strips with say <010> or <x1x> pattern will be performed. However due to byte alignment requirements this alone would not reduce the data volume.

There are several other things which could also be done in the ROB:

- Clustering of adjacent strips into clusters if not already done by the ROD.
- Conversion of chip/strip address into r-phi or z-phi coordinates using a look up table.
- Space point finding using normal-stereo association and production of 3-dimensional r-phi-z coordinates.
- Using 3-dim space points, further data selection may be performed to check that the 3-dim coordinate is within the ROI region.

These processing steps have been studied and details can be found in *[9]*.

The output format may therefore be a list of module/chip/strip addresses corresponding to each cluster, or a list of ATLAS 2- or 3-D coordinates. It is however not clear that these will lead to any great reduction in data volume.

Figure 3: Layout of SCT barrel ladders.

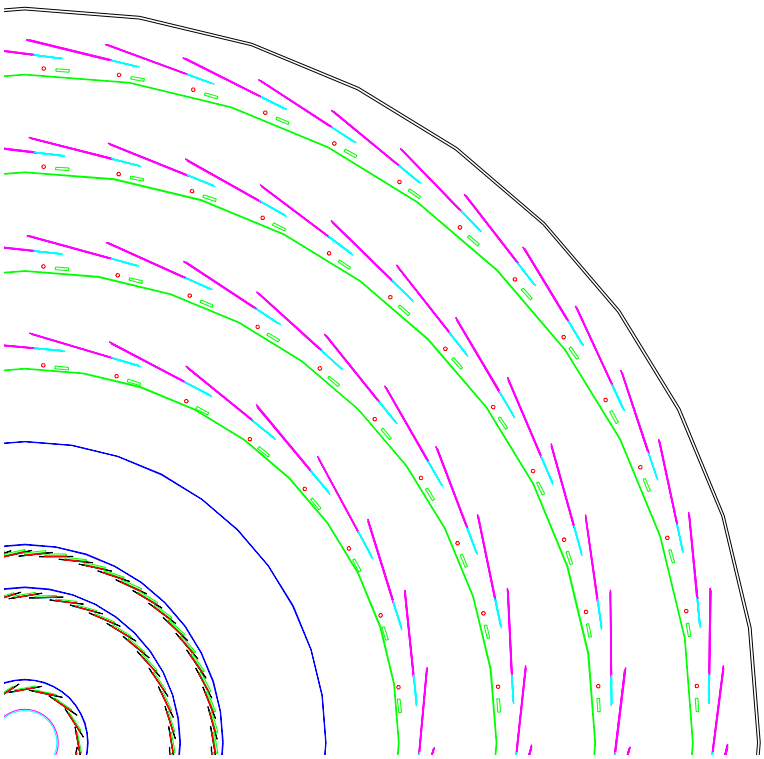

Figure 4: Layout of inner detector showing SCT barrel and endcap wheels.

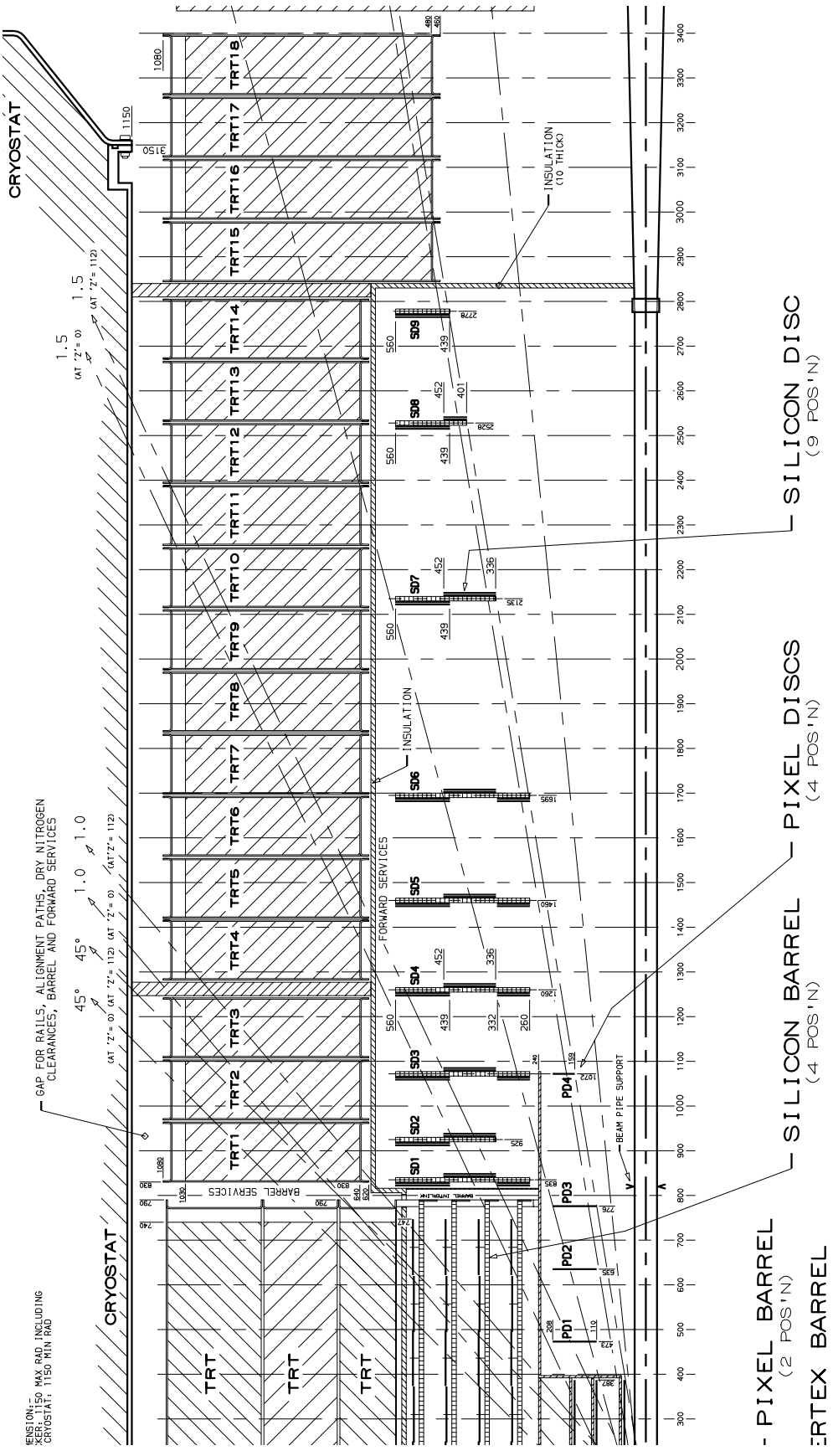

4 The Pixel Detector

Most details given in this section are taken directly from the Pixel TDR document *[10]*.

4.1 Modules

The basic unit of the pixel detector is a mechanical module. The modules used in the barrel and discs are essentially identical. A module is constructed from 16 pixel chips [1] arranged to give a module of sensitive area 16.4mm x 60.4mm, containing 320 (ϕ direction) x 192 (z or r direction for barrel or endcap respectively) pixels (61440 in total). The pixel dimension is 50μm(ϕ) x 300μm(z or r). The module contains one module-control-chip which collects data from the 16 pixel chips, and serves as the point of contact for readout. Therefore a pixel within a module is identified locally by Chip/Row/Column.

4.2 Geometry

There are three barrel layers, the innermost being a replaceable vertex layer (also known as the B-layer). Within each layer modules are mounted in rows on ladders (staves). Each ladder runs in the z direction and contains 13 modules, the ladders repeating around the ϕ direction. The geometry and number of modules is given in table 6 below. The approximate η range is 1.7 (2.5 for the vertex layer).

There are five identical endcap discs at each end. Each ring contains a single ring of 72 modules running around in ϕ. The geometry and number of modules is given in table 7 below. Mechanically the discs are formed from twelve “sectors” each containing 6 modules. The endcap covers the approximate range $1.7 < \eta < 2.5$.

The total number of channels in the barrel and both endcaps combined is 1.4×10^8.

Layer	Radius (mm)	z range (mm)	#ladders (in ϕ)	#modules on ladder	#modules in layer	Channels (61440/mod.)
Vertex	*43*	*+- 389*	*18*	*13*	*234*	*1.4×10^7*
Middle	*101*	*+-389*	*42*	*13*	*546*	*3.4×10^7*
Outer	*132*	*+-389*	*56*	*13*	*728*	*4.5×10^7*
Total					**1508**	*9.3×10^7*

Table 6: Pixel Barrel: Geometry, module and channel count.

1. Each chip has 160 (ϕ) x 24 (r or z) pixels. These are arranged in a 2 x 8 grid to give a module having 320 (ϕ) x 192 (r or z) pixels.

Disc	r range (mm)	z (mm)	#modules	Channels (61440/mod.)
1	*126-187*	*495*	*72*	*4.4×10^6*
2	*126-187*	*612*	*72*	*4.4×10^6*
3	*126-187*	*670*	*72*	*4.4×10^6*
4	*126-187*	*841*	*72*	*4.4×10^6*
5	*126-187*	*926*	*72*	*4.4×10^6*
Total (x 2 ends)			**360 (720)**	*2.2×10^7 (4.4×10^7)*

Table 7: Pixel Endcap: Geometry, module and channel count.

4.3 Readout Segmentation

At present the best model is that the Pixel modules will be read out in the same fashion as the SCT, i.e. there will be two data fibres and one control fibre per module. These fibres will go directly to the ROD.

The grouping of fibres into ribbons (particularly for the barrel where the 13 module count presents a problem) is still under development and therefore no firm statement can be made at this point. A natural grouping of fibres would result in a "6-module set" being read out via one set of optical connectors and hence becoming the minimum unit of readout (MUR). This occurs if 12 data fibres end in a 12-way MT12 connector and the corresponding 6 control fibres end in a 6-way MT6 optical connector.

In the endcap this MUR would make a perfect match to the mechanical segmentation into sectors containing 6 modules. In the barrel this would result in the MUR being a "nearly" half ladder, but leaves the problem of the odd 13th module (which could for instance be read out via its own separate 4-way fibre ribbon to carry both data and control).

For the purposes of this document we make the assumption that the MURs are the 6 module sets as outlined above. Further, we will for now finesse the barrel odd 13th module problem by assuming that it can always effectively be grouped into the same ROD as one of its half ladders. This would introduce an asymmetry in the rates.

The number of modules which could be fed into a single ROD may be up to 48 [1] (same as SCT), or equivalently 8 MURs. The revised mapping *[11]*, however, has 6 MURs per ROD for the outer two barrel layers and only 1 MUR per ROD for the inner, vertex layer. The number of modules mapped into a ROD is limited by the occupancies and the readout link bandwidth to the ROB.

1. This depends on whether time-over-threshold information is sent. If it is sent then each hit pattern takes 25 bits and only about half the modules can be concentrated into a single ROD due to data volume limitations. If this information is not sent then each hit pattern can be put into 16 bits leading to roughly half the data volume. We assume the latter here.

There will be two flavours of Pixel ROD, one for the B-layer (supporting maybe 6 modules) and one for the outer barrel (supporting maybe 36 modules) and endcaps. The mapping of modules into the latter flavour should probably not be mixed between barrel and endcap. The grouping of MURs into RODs is the subject of the same studies *[5][11]* as required for the SCT.

For the purposes of this document we assume the following:

In the barrel vertex layer, individual MURs are used. The inner barrel is therefore divided into 18 ϕ segments per half barrel (18 half ladders), giving 36 RODs.

In the outer barrel, MURs from the two layers are grouped to form projective wedges with approximately equal ϕ segmentation. The outer barrel is therefore divided into 16 ϕ segments per half barrel (98 half ladders divided into sets of 6, except for two sets of 7) giving 32 RODs.

In the endcap, MURs from each of the 5 discs are grouped together in the following two alternating patterns: *a* {1+1+2+2+2} = 8 MURs, and *b* {2+2+1+1+1} = 7 MURs (the numbers indicate the number of MURs taken from each of discs 1-5). These two patterns therefore 'interlock' and are repeated around the disc *ababab*.... This yields 8 RODs per endcap.

The mapping into RODs is summarised in table 8. This mapping yields 84 ROBs for the entire Pixel detector.

Pixel readout segmentation into a single ROD. (undecided, these are some options)	$\Delta\phi$	η	**channels/ ROD**	**#RODs**
Inner Barrel: B-layer one half ladder	*0.4*	*~0.0-2.9*	*3.7 x 10^5*	***36***
Outer Barrel: 6 half ladders from outer 2 layers in approximate projective geometry	*~0.5*	*~0.0-1.8*	*2.2 x 10^6*	***32***
Endcap: 5 projective "octants" from successive wheels	*~1.0*	*1.7-2.7*	*2.8 x 10^6*	***8 x 2***

Table 8: Pixel readout segmentation into RODs.

4.4 Occupancy

The occupancy is approximately 10^{-4} per pixel, everywhere except the vertex barrel layer which is 5.10^{-4} at high luminosity [Inner Detector TDR, Volume 1, Table 3-14, p81]. Inside high-p_T b-jets the occupancies are 3.10^{-4} and 5.10^{-4} respectively. The occupancy due to minimum-bias pile-up at low luminosity is $1.1.10^{-5}$ (5.10^{-5} in the B-layer), including an occupancy due to noise of 1.10^{-6} [Pixel TDR, Table 5-1, p71].

The cluster size (defined as pixels adjoining in any manner) is somewhere around 2-4 for all modules.

These figures translate to 6 pixel hits/module/event for pile-up events, corresponding to 2-3 clusters/module/event (30 pixel hits/module/event in the vertex layer).

4.5 Data into ROD

The format of the data into the RODs is now almost certainly fixed *[7]*. Under normal running conditions the readout chips on the modules only transmit information for hit pixels. Apart from headers and trailers the basic pixel information consists of 4+8+5 bits for FE-chip/Row/Column respectively (8 bits would be added for time-over-threshold).

This yields approximately 10-15 kbits/ROD/event at high luminosity. The corresponding number at low luminosity is 1-2 kbits/ROD/event.

4.6 Data from ROD to ROB

In principle the basic hit information is 17 bits which is inconvenient. However the Pixel group have proposed a simple trick to reduce it to 16 bits. The idea is to reduce the number of chip address bits from 4 to 3 by sending a 'half module' header following every 8 chips (there are 16 chips on a module). In this case the data format is:

for each half module: <header><mmmmmmmmmmmmm> (16 bits)

then

for each hit pixel: <fff><rrrrr><cccccccc> (16 bits)

where:

<mmmmmmmm> is a unique 13-bit module number (byte aligned to 16 bits)
<fff> is the reduced 3-bit FE chip number within a module
<rrrrrrrr> is the 8-bit row number
<ccccc> is the 5-bit column number

Using the occupancies stated earlier gives [1] 180 hit pixels/ROD/event in the inner barrel, 216 hit pixels/ROD/event in the outer barrel and 270 hit pixels/ROD/event in the endcaps. This yields [2] **3.4 kbits/ROB/event** in the inner barrel, **4.9 kbits/ROB/event** in the outer barrel and **6.1 kbits/ROB/event** in the endcap, for the case of high luminosity. For low luminosity, the corresponding numbers are about a factor of 10 lower.

---

1. The calculation assumes the endcap and outer barrel modules contributing to a ROD have 6 hits/event (@ 10^{-4} occupancy) and the inner barrel modules have 30 hits/event (@ 5.10^{-4} occupancy).
2. The calculation assumes 2x16 half-module identifier bits + n x 16 data bits per module/event, where n = the number of hits per module. To this is added 10 32-bit words for the fragment header.

4.7 Data from ROB to FEX

Exactly the same discussion as presented for the SCT is applicable. The ROB may perform any of the following:

It may be useful to select ROI data. However in the barrel vertex layer this will not help much as the ROI size in η is very large (due to the interaction point extent in z). The reduction factor may be up to 10.

Clustering of adjacent pixels if not already done by the ROD.

Conversion of address into 3-D coordinates using a look up table.

It is assumed that no significant data reduction results apart from the data selection factor.

5 Calorimeters

The content of this chapter is to describe the “first order mapping” of the calorimeter ROD-ROB assuming a one-to-one correspondence and based of the present knowledge of the front end electronics LARG and TILES calorimeters. However, assumption and simplification has been made in order to unify the various parameters listed below.

Number and mapping of ROBs in Eta-Phi space

Data production and format from each FEB and ROD to ROB

5.1 Geometry and trigger segmentation

The calorimeter is divided into two subsystems:

The Liquid Argon (LARG) Calorimeter electromagnetic (EM), Hadronic End cap (HEC) and forward (FCAL).

The Hadronic tile (TILE CAL) calorimeter

Tables 9 and 10 show the segmentation in LVL1 Trigger Tower (TT) and the total number of channels in function of eta for the various partitions.

Eta	EtaxPhi	TT	Tot Ch
0 - 1.4	0.1 x 0.1	1792	107520
1.4 - 1.47	0.1 x 0.1	128*	2688
Barrel			**110208**
1.4 - 1.5	0.1 x 0.1	128*	2560
1.5 - 1.8	0.1 x 0.1	384	23040
1.8 - 2.0	0.1 x 0.1	256	12288
2.0 - 2.4	0.1 x 0.1	512	20480
2.4 - 2.5	0.1 x 0.1	128	3584
2.5 - 3.1	0.2 x 0.2	192	1536
3.1 - 3.2	0.2 x 0.2	64	256
End Cap			**63744**
Total		**3456**	**173952**

Table 9: Larg EM Trigger Tower Segmentation

HEC			Tot Ch
1.5 - 1.6	0.1 x 0.1	128	256
1.6 - 2.5	0.1 x 0.1	1152	3456
2.5 - 3.1	0.2 x 0.2	192	576
3.1 - 3.2	0.1 x 0.2	64	192
			4480
FCAL			
3.2 - 4.9	0.2 x 0.2	64	**11288**
Total		**1600**	

Table 10: Larg HEC and FD calorimeter Trigger Tower segmentation

5.2 The LARG Readout Chain

Signals from each detector cells are processed by various stages before being delivered to the ROB:

5.3 The Front End Board (FEB)

This first module perform the following tasks:

amplify and shape the analog cell signals

sum the calorimeter cells by trigger tower within each depth layer, and prepare the input signals for the tower builder board

store the signals in an analog memory (SCA) waiting for the decision of the first level triggering.

digitize the selected pulses.

transmit on optical fibres the multiplexed digital results.

These FEB's are housed "on-detector", in a front end crate attached to the cold to warm feedthroughs, in a crack between the barrel and the end-cap calorimeters and at the rear of the end caps. The data from the FEB boards are pushed to the optical fibers in a serial mode of 1.28 Gb/s and a mean rate of the LVL1 trigger: nominal 75 KHz, upgradable to 100KHz, with few percent dead time. Each FEB is serving 128 calorimeter channels from the same feedthrough and the same calorimeter layer. There are 16 x 12 bit ADC, one for 8 channels. The digitized data are send to the next module: the Read-Out Driver (ROD) using a 32 bit word at 40 MHz. At each clock cycle two bit from the each ADC are send (2bit per ADC x16 ADC's = 32 bits), and 8 cycles are needed to send the complete digitization (12bit from ADC + 4 bits for the gain and parity). Thus the time to send one digitization is 8 cycles of 25ns=200ns, and therefore for the complete 50 words of each event (8 channels per ADC x 5 timing samples + headers) 10µsec are needed.

5.3.1 The Readout Driver (ROD)

The basic function of the second module of the read-out chain are:

receive and buffer data from the FEBs.

calculate the energy and time and extract some form of data quality flag for each channel.

monitor and calibrate data

format and send the data to the ROB

In the baseline architecture for the system *[12]*, there is two-to-one correspondence between the FEB and the ROD module i.e. 256 channels per ROD. Each ROD board will consist of eight DSP Processing Units, with a pre-defined number of channels (64). Because of the amount of buffering needed in the ROD modules, the maximum event latency is expected to be 80 x 10 µs = 800 µs.

5.4 Larg ROD (ROB) baseline (layer) mapping

5.4.1 Larg EM

Tables 11, 12, 13 and 14 show this "layer" mapping that details the number of cells per Trigger Tower, the number of channels in each layer and finally the ROD number as a function of Eta for the Larg EM calorimeter The barrel is built from two halves, each covering roughly the eta rapidity range up to 1.4. In azimuth, each half barrel is physically made of 16 independent supermodules. The calorimeter has effectively 4 layers in depth: presampler, front layer (preshower) middle layer and back layer. The two end caps are built from two wheels: the outer (1.4<eta<3.2) and the inner (2.4<eta/<3.2) wheels. The calorimeter has 3 to 4 layers in depth depending on the eta. There is a great deal of flexibility in assigning FEBs to RODs. In the example, it is chosen to assign, where possible, FEBs treating a given layer to a given ROD. It should be noticed that the mapping should respect the feedthrough topology (64 in the barrel, 32 standards and 2 special in the end cap): some ROD can map only one FEB instead of 2 (example in the Barrel front layer). If the situation in the Barrel is quiet stable, the assignment in the end cap may evolve and change slightly: the present mapping is presented as a "first realistic order".

24-avr-99 v 2.0			**Presampler**				
Eta	**EtaxPhi**	**TT**	**Cells/TT**	**Channels**	**ROD (EtaxPhi)**	**TT/ROD**	**ROD**
0 - 1.4	0.1 x 0.1	1792	4	7168	1.5 x 0.4	60	32
1.4 - 1.47	0.1 x 0.1	128	5	640		combined with above	
Total Barrel		**1920**		**7808**			**32**
1.5 - 1.6	0.1 x 0.1	128	4	512	0.1 x 1.6	16	8
1.6 - 1.8	0.1 x 0.1	256	4	1024	0.2 x 1.6	32	8
Total End Cap		**384**		**1536**			**16**
Total		**2304**		**9344**			**48**

Table 11: ROD mapping of the Larg EM presampler layer

22-avr-99v 2.0		Front					
Eta	EtaxPhi	TT	Cells/TT	Channels	ROD (EtaxPhi)	T/ROD	ROD
0 - 1.2	0.1 x 0.1	1536	32	49152	0.4 x 0.2	8	192
1.2 - 1.4	0.1 x 0.1	256	32	8192	0.2 x 0.2	4	64
1.4 - 1.47	0.1 x 0.1	128	12	1536		combined with above	
Total Barrel		**1920**		**58880**			**256**
1.4 - 1.5	0.1 x 0.1	128	4	512	0.1 x 1.6	16	8
1.5 - 1.8	0.1 x 0.1	384	32	12288	0.1 x 0.8	8	48
1.8 - 2.0	0.1 x 0.1	256	24	6144	0.1 x 0.8	8	32
2.0 - 2.4	0.1 x 0.1	512	16	8192	0.2 x 0.8	16	32
2.4 - 2.5	0.1 x 0.1	128	4	512	0.1 x 1.6	16	8
2.5 - 3.1	0.2 x 0.2	192	4	768	0.7 x 3.2	64	4
3.1 - 3.2	0.2 x 0.2	64	2	128		combined with above	
Total End Cap		**1664**		**28544**			**132**
Total		**5376**		**87424**			**388**

Table 12: . ROD mapping of the Larg EM Front layer

22-avr-99 v2.0		Middle					
Eta	EtaxPhi	TT	Cells/TT	Channels	ROD (EtaxPhi)	TT/ROD	ROD
0 - 1.2	0.1 x 0.1	1536	16	24576	0.4 x 0.4	16	96
1.2 - 1.4	0.1 x 0.1	256	16	4096	0.3 x 0.4	12	32
1.4 - 1.47	0.1 x 0.1	128	4	512		combined with above	
Total Barrel		**1920**		**29184**			**128**
1.4 - 1.5	0.1 x 0.1	128	16	2048	0.1 x 1.6	16	8
1.5 - 1.8	0.1 x 0.1	384	16	6144	0.1 x 1.6	16	24
1.8 - 2.0	0.1 x 0.1	256	16	4096	0.1 x 1.6	16	16
2.0 - 2.4	0.1 x 0.1	512	16	8192	0.2 x 0.8	16	32
2.4 - 2.5	0.1 x 0.1	128	16	2048	0.1 x 1.6	16	8
2.5 - 3.1	0.2 x 0.2	192	4	768	0.7 x 3.2	64	4
3.1 - 3.2	0.2 x 0.2	64	2	128		combined with above	
Total End Cap		**1664**		**23424**			**92**
Total		**5376**		**52608**			**220**

Table 13: ROD mapping of the Larg EM Middle layer

22-avr-99 v 2.0		Back Layer					
Eta	**EtaxPhi**	**TT**	**Cells/TT**	**Channels**	**ROD (EtaxPhi)**	**TT/ROD**	**ROD**
0 - 0.8	0.1 x 0.1	1024	8	8192	0.8 x 0.4	32	32
0.8 - 1.4	0.1 x 0.1	768	8	6144	0.6 x 0.4	24	32
Total Barrel		**1792**		**14336**			**64**
1.5 - 1.8	0.1 x 0.1	384	8	3072	0.1 x 3.2	32	12
1.8 - 2.0	0.1 x 0.1	256	8	2048	0.1 x 3.2	32	8
2.0 - 2.4	0.1 x 0.1	512	8	4096	0.2 x 1.6	32	16
2.4 - 2.5	0.1 x 0.1	128	8	1024	0.1 x 3.2	32	4
Total End Cap		**1280**		**10240**			**40**
Total		**3072**		**24576**			**104**

Table 14: ROD mapping of the Larg EM Back layer

Figure 5: Presampler Mapping.

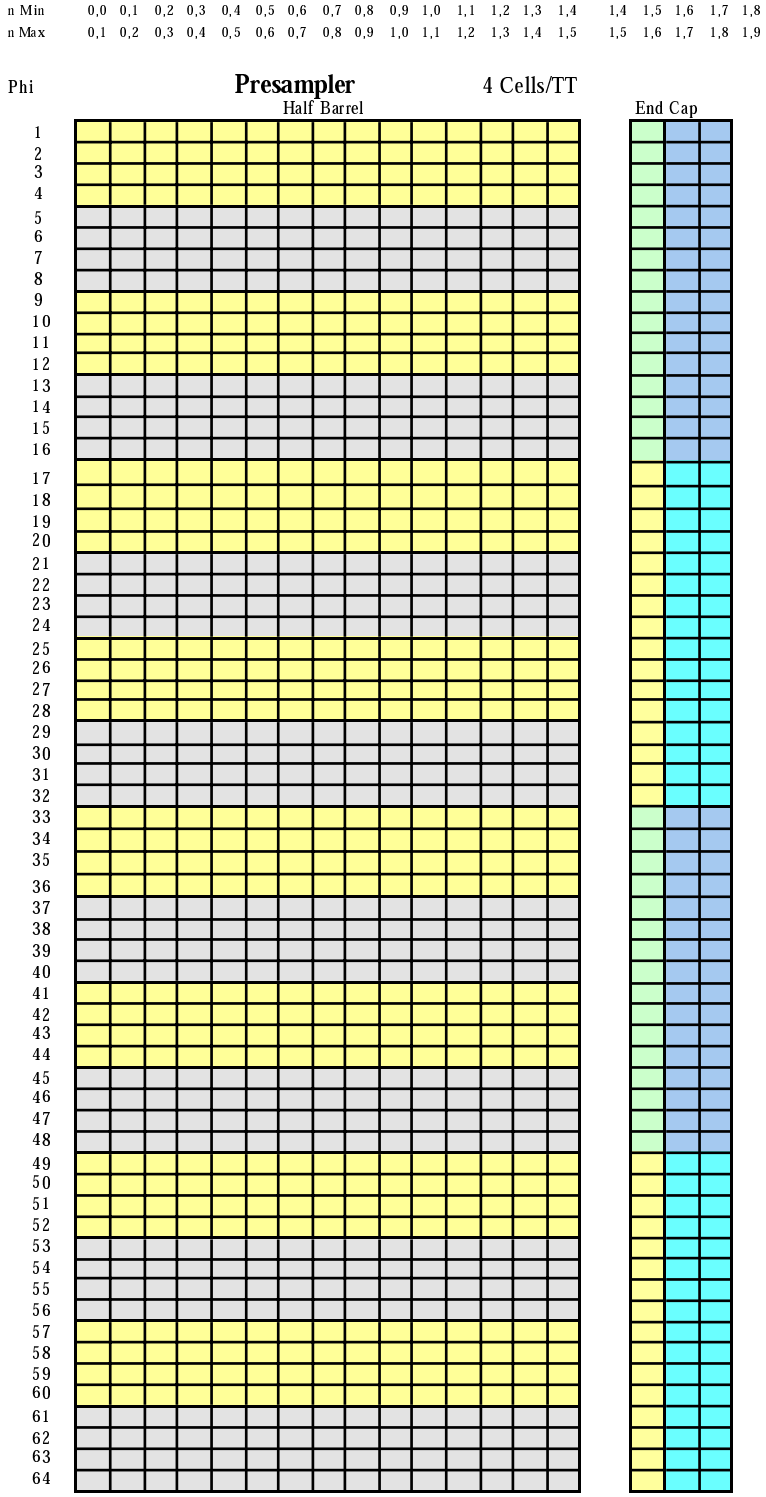

Figure 6: EM Front Layer Mapping.

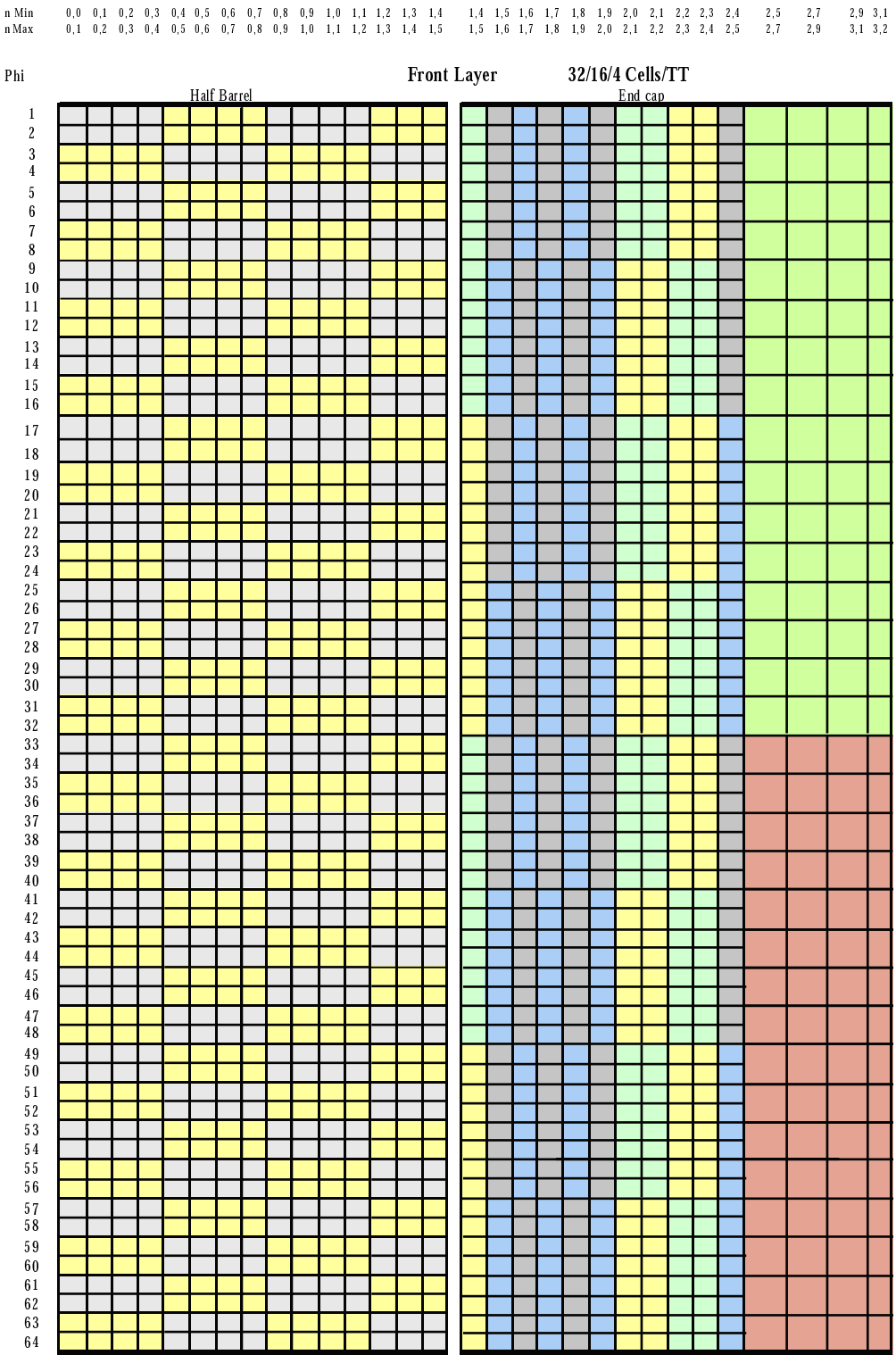

Figure 7: EM Middle Layer Mapping

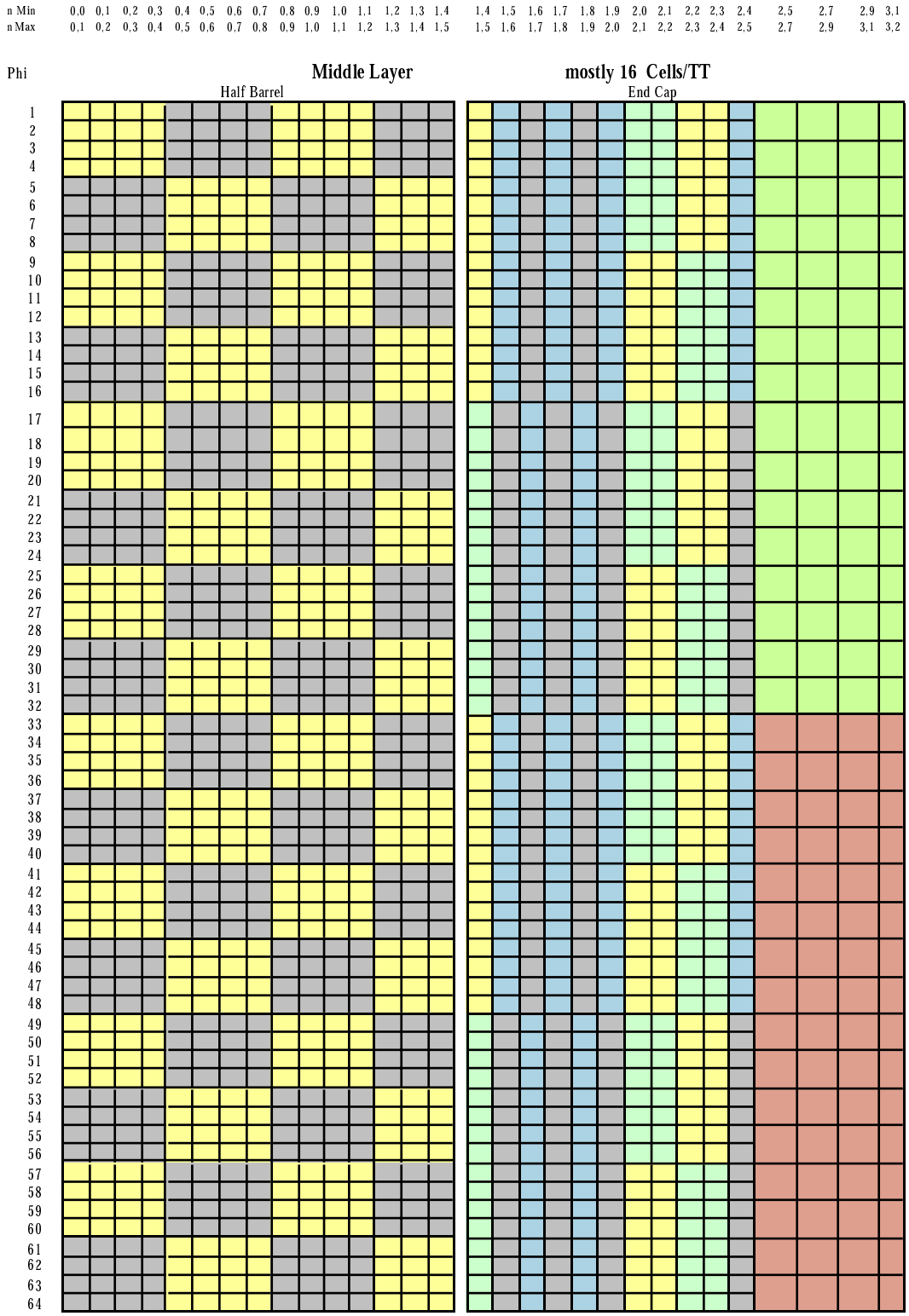

Figure 8: EM Back Layer Mapping

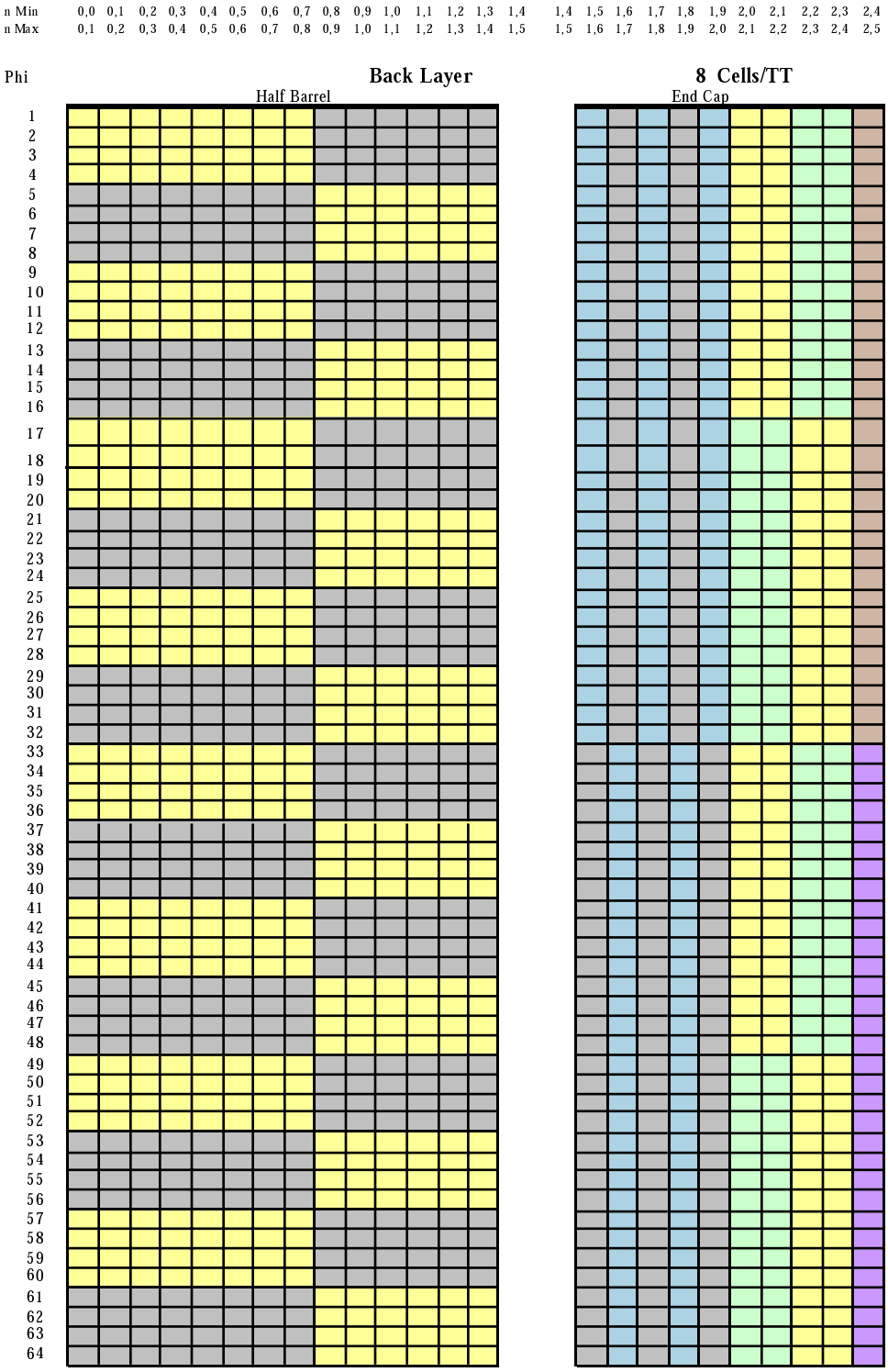

5.4.2 Larg HEC

Table 15 shows the mapping of the Larg HEC using one cell per TT and the assumption that the same ROD packaging (256 ch) are used. Each of the two hadronic end cap are built from two wheels (front and back wheels) for a total of 3 layers in depth.

22-avr-99 v 2.0		HEC Front & Middle					
Eta	EtaxPhi	TT	Cells/TT	Channels	ROD (EtaxPhi)	TT/ROD	ROD
1.5 - 1.6	0.1 x 0.1	128	1	128	0.1 x 6.4	64	2
1.6 - 2.5	0.1 x 0.1	1152	1	1152	0.9 x 1.6	144	8
2.5 - 3.1	0.2 x 0.2	192	1	192	0.7 x 6.4	128	2
3.1 - 3.2	0.1 x 0.2	64	1	64		combined with above	
Total Barrel		1536		1536			12
HEC Back Layer							
Eta	EtaxPhi	TT	Cells/TT	Channels	ROD (EtaxPhi)	TT/ROD	ROD
1.5 - 1.6	0.1 x 0.1	128	1	128	0.1 x 6.4	64	2
1.6 - 2.5	0.1 x 0.1	1152	1	1152	0.9 x 1.6	144	8
Total Barrel		1280		1280			10
Total		4352		4352			34

Table 15: ROD mapping of the Larg HEC calorimeter

5.4.3 Tower Mapping Option

This second option proposed in a first study have the advantage of building directly the full trigger tower at the ROD level but the disadvantage of a complex connection between FEB to ROD.

Recent studies of a LVL2 sequential (layer) treatment of the calorimeter algorithm may decrease the interest of that solution. In table 16 it is assumed that each ROD treats up to 4 Trigger Towers (eta-phi coverage of 0.2 x 0.2) compatible with a ROD of 256 channels.

Barrel	512
Standard End Cap	256
Special End Cap	70
Total ROD/ROB	838

Table 16: Large EM ROD "Tower Mapping"

Figure 9: ROD Mapping of the Larg HEC Calorimeter.

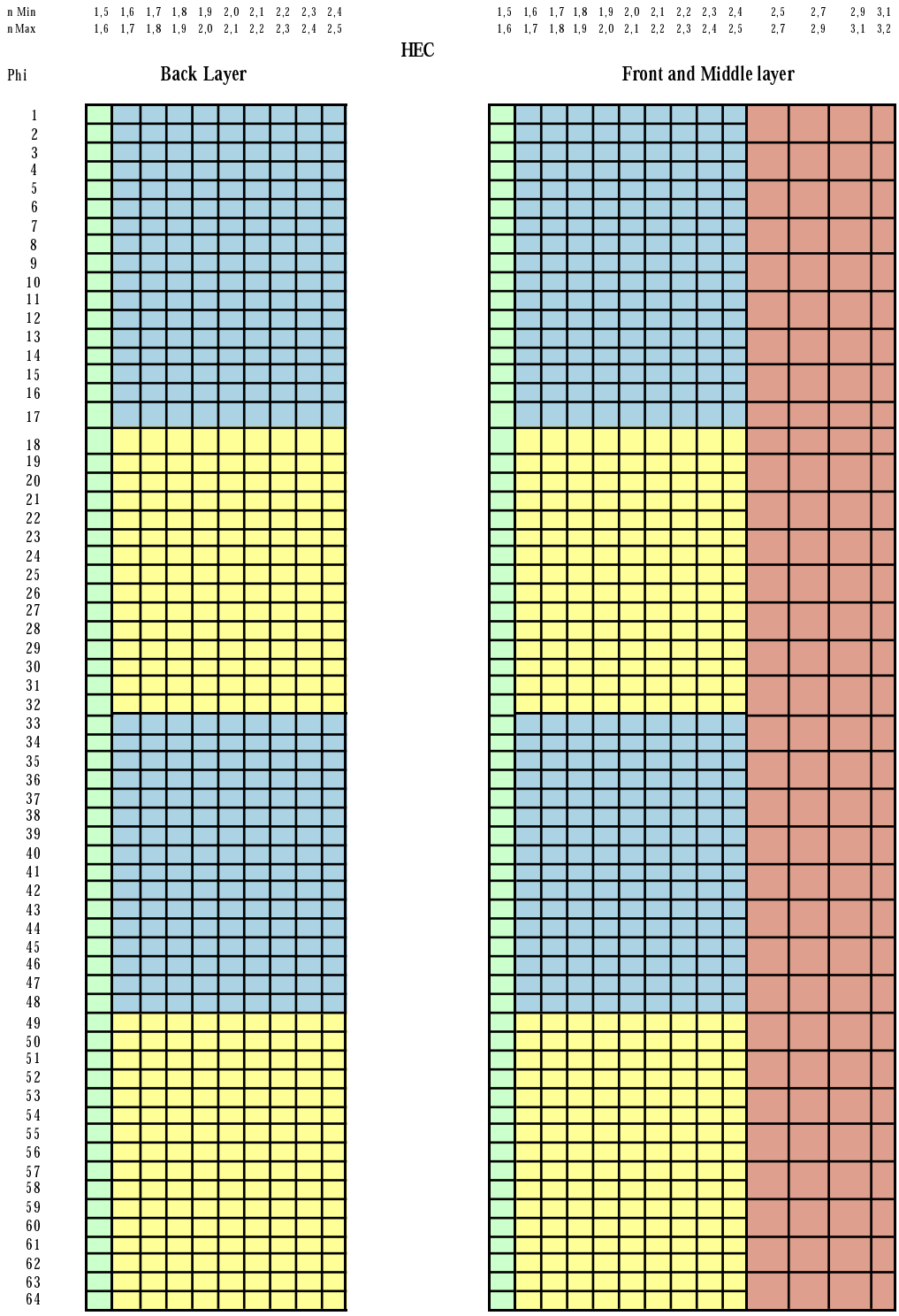

5.5 The Hadronic Tile barrel & extended barrel

The hadronic tile calorimeter is mechanically divided into three physical parts: one central barrel up to eta < 1.4 and an extended barrel on each sides up to eta=1.6, the later separated by gaps from the central barrel. In azimuth, each piece is made of 64 wedges, which are grouped by four to give 16 readout supermodules. There are three logical layers in depth, obtained from four physical layers by grouping the 2 external layers into a single readout channel. As the cells are bounded by planes of constant z, the coverage in delta eta is approximate.

5.5.1 Tile Calorimeter Front End Drawer

Tile Cal is instrumented by drawers containing the front-end electronics (Shapers, Level1 adders, Bigain system and digitizers) as well as the Calibration system (Integrator, Charge injection). Each drawer is defined and designed as a stand alone Read out Item. Following a L1A rate of 75 KHz expected bandwidth per link is 330 Mb/s for the barrel part and 205 Mb/s for the Extended part. In both cases the Header data fraction is 30/70%.

5.6 Tile Calorimeter Baseline Read Out Driver

The baseline follows mainly the LARG philosophy:

Data coming from each digitizer is processed and buffered in a FIFO memory in a first step. The data needs to be reordered to extract the BCID number as well as the individual samples

The Shape Waveform Analysis will guide the processing of the buffered data, to the Pile-Up, Empty or Energy and Timing algorithms.

Energy and Timing value are calculated in a DSP using a linear combination of the input samples.

A confidence factor for T and E are estimated.

Format and multiplex output data to prior to be send to the ROB link.

5.6.1 Tile Calorimeter ROD (ROB) mapping

The baseline maps four drawers to one ROD modules so that a complete TileCal sector can be linked to a single ROD. Complete TileCal Read out is 256 drawers, therefore 64 ROD (ROB) are needed. This information is summarized in table 17.

22-avr-99 v 2.0			Tiles					
Eta	EtaxPhi	TT	Drawer	Ch/Drawer	Channels	ROD (EtaxPhi)	TT/ROD	ROD
0 - 1.4	0.1 x 0.1	1792	128	46	5888			
1.4 - 1.6	0.1 x 0.1	256	128	31	3968			
Total Barrel		**2048**			**9856**	**3.2 x 0.1**	**32**	**64**

Table 17: Summary of TileCal parameters

Figure 10: TileCal ROD Mapping.

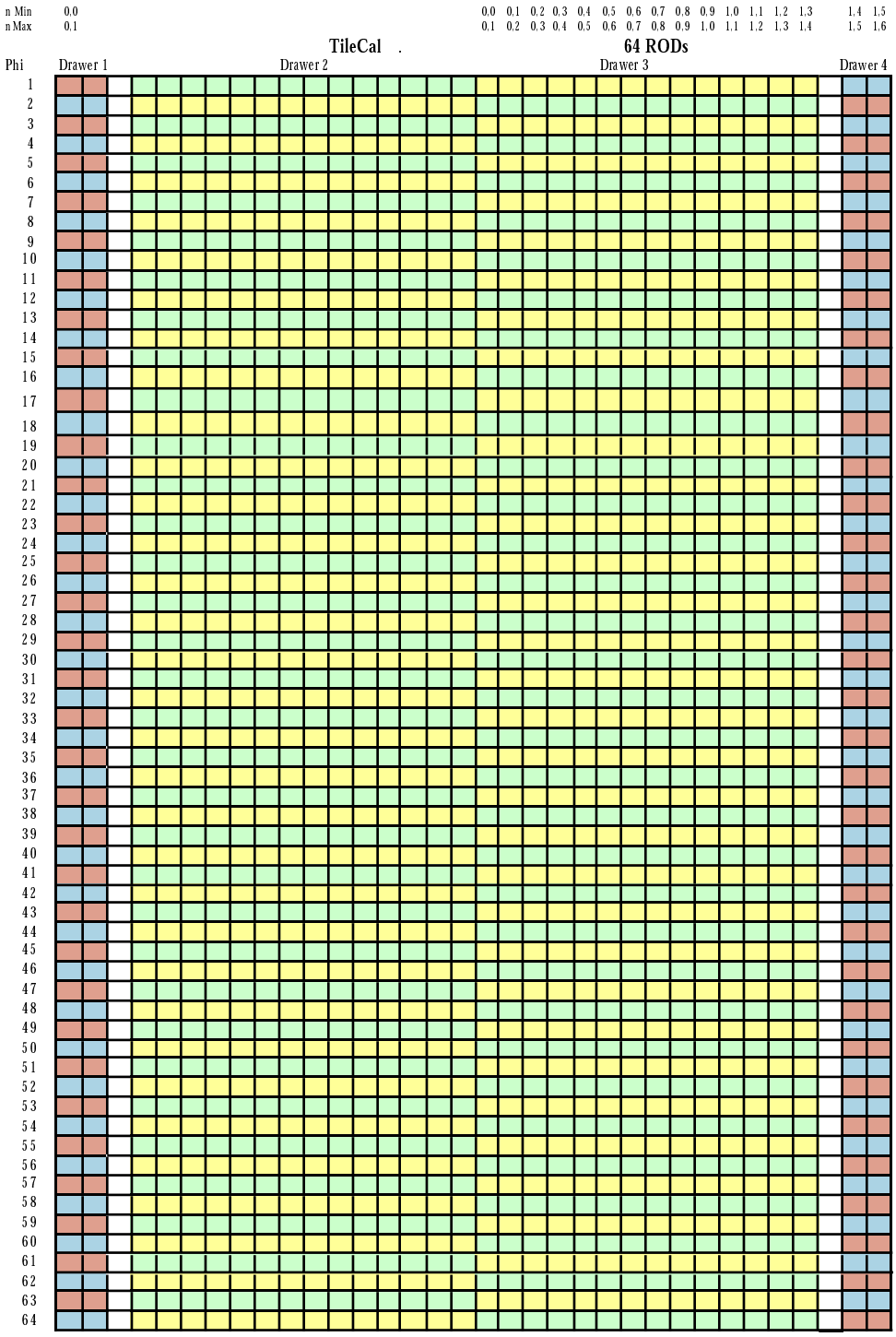

5.7 Calorimeter data format & production from RODs

There is no zero suppression at the ROD level. Tables 18 and 19 show an estimate of this format in the case where no raw data are sent to the Larg and TILECAL ROB. Table 18 shows an estimate of the ROD data production in the Larg assuming a LVL1 rate of 75 kHz and 32 bit words for the different data blocks in the event fragment.

Block	Detector Block	Length	Maximum Size	Typical Size
#0	Header & Control Words	Fixed	12	12
#1	Trigger Tower Sums	Fixed	5	5
#2	Energy & Coarse Time	Fixed	384	384
#3	Precise Time & Quality of Fit	Variable	256	28
#4	Raw Data Information	Variable	768	20
#5	Read Addresses	Fixed	80	0
	Total (32 bit words)		**1505**	**449**

Table 18: Larg typical event size

Note:

The typical size is calculated assuming that:

~10% of the channels have energy above threshold for which the precise time needs to be calculated.

~1% of the channels have high energy for which the raw data need to be available for normal running, there is not need to output the ROD words in each event.

LVL1=75KHz	TileCal
Header	16
Energy and quality flag	154
Time	52
Status summary	3
Total (32 bit word)	225
Bandwidth (Gbit/s)	0.54

Table 19: Estimated Tilecal ROD data output

6 Precision Muon Chambers

The overall layout of the muon chambers in the ATLAS detector is shown in figure 11. It indicates the different regions where four different chamber technologies are employed: MDTs and CSCs are used for precision measurements and RPC and TGC for trigger purposes. MDTs and RPCs are used in the barrel region and MDTs, CSCs and TGCs in the endcaps. The side view of a half detector is shown in figure 12. It also indicates the detector segmentation in pseudorapidity intervals.

6.1 Geometry

The precision muon chamber structure is rather complex, being assembled from many different types of chambers (in the barrel alone there are 12). It is inappropriate for the purpose of this document to repeat the details of the geometry which can be found in the Muon TDR*[13]*. Therefore a simplified approximation is given which contains all the details relevant to data flow. The numbers quoted in the text refer to the layout called M.4. A summary of precision chamber parameters is reported in tables 20 and 21.

MDT	Barrel			Endcap	Total
	Standard	Special	total		
#chambers	560	122	682	512	1194
#tubes	174,816	31,296	206,112	165,120	371,232

Table 20: Summary of precision chamber module and tube count

CSC	Small	Large	Total
#chambers	16	16	32
#wires	35,840	55,296	91,136
#strips	30,720	30,720	61,440

Table 21: Summary of CSC chamber, wire and strip count.

6.1.1 Barrel

The barrel covers the pseudorapidity range $|\eta| < 1$. MDT chambers form three concentric rings made of odd sectors of *large* chambers and even sectors of *small* chambers. There are therefore two basic ϕ segmentations, 0.52 and 0.26 radians respectively (30 and 15 degrees). The transverse view of the spectrometer and the definition of sectors is shown in figure 13. Standard sectors are 1-10 and 16, special sectors are 11-15, which are located in the region of the magnet feet and the calorimeter rails. The outer, middle and inner sets of chambers are called outer, middle and inner stations respectively (BO, BM and BI, where B means barrel).

In the barrel, the chambers are arranged in projective towers as shown in figure 12. The MDTs consist of two multilayers of drift tubes separated by a spacer and a support structure (see figure 14). Each multilayer consists of three (outer and middle stations) or four (inner station) layers of 3 cm diameter drift tubes. In each chamber the tubes run along the direction of the toroidal field (ϕ direction); the number of tubes per chamber varies along the z direction and the total number of tubes, together with layout details, are reported in table 22.

6.1.2 Endcap

MDTs are used for the precision measurements in the endcaps over most of the area, with the CSCs covering the high rate region, $|\eta| = 2\text{-}2.7$, in the inner station.

The endcap MDTs cover the pseudorapidity range $|\eta| = 1\text{-}2.7$. On each side of the detector they are arranged in four rings, concentric with the beam axis. The chamber planes are orthogonal to the beam axis with the drift tubes running in the same direction as in the barrel. The MDTs are arranged with the same 16-fold segmentation in azimuth of the barrel, with *large* and *small* chambers covering the same azimuthal ranges as the barrel ones. The second MDT ring (station EE, where E means endcap) covers the so called *transition* region. The remaining three rings form the stations EI (endcap inner), EM (endcap middle) and EO (endcap outer).

The endcap MDTs are of trapezoidal form with tapered edges (layout M). As a consequence the length of the individual tubes within one layer changes from tube to tube. In the last chamber layout (N), which is not considered here, the tubes are grouped by 8 within the same layer and built of the same length. Channel count, segmentation and details of the endcap geometry are summarized in table 23.

Station	**Approx Radius** at large chamber centre **(mm)**	**Approx z range (mm)**	**segmentation in ϕ** (half are large and half are small)	**#tubes in z (approx) x #layers (per segment)**	**Total #channels**
inner (BI)	*4900*	*+- 6500*	*16*	*430 x 8*	*6.9×10^4*
middle (BM)	*7100*	*+-9100*	*16*	*600 x 6*	*5.4×10^4*
outer (BO)	*9500*	*+-12200*	*16*	*800 x 6*	*8.3×10^4*
Total					***21×10^4***

Table 22: Muon MDT Barrel: Geometry, module and channel count. Numbers are given for standard sectors in most cases.

'Wheel'	Approx η range (mm)	segmentation in ϕ (half are large and half are small)	#tubes in r (approx) x #layers (per segment)	Total #channels
inner EIS+EIL	*EIL:1.07-2.03 EIS:1.36-1.93*	*16*	*130x8*	*1.7×10^4*
transition EES+EEL	*EEL:1.07-1.36 EES:1.03-1.36*	*16*	*90x6*	*0.9×10^4*
middle EMS+EML	*EML:1.07-2.70 EMS:1.03-1.36*	*16*	*310x6*	*3.0×10^4*
outer EOS+EOL	*EOL:1.36-2.70 EIO:1.36-2.71*	*16*	*310x6*	*3.0×10^4*
Total (x 2 ends)				***8.6×10^4*** *(17.2×10^4)*

Table 23: Muon MDT endcap geometry and channel count.

6.2 Readout segmentation

A typical chamber station is shown in figure 14. Presently the MDT readout electronics include:

a pre-Amplifier, Shaper, Discriminator (ASD) and a simple ADC which are contained within a custom 8-channel CMOS IC. The output of three ASD chips drives a 24-channel TDC. Three ASDs and one TDC are mounted on a single mezzanine card which handles 24 channels. In the middle and outer chambers this corresponds to 8 tubes x 3 layers, in the inner chambers to 6 tubes x 4 layers. Figure 14 shows the numbering convention within a MDT chamber;

the mezzanine board uses one FE-link to move data from the TDC into a Chamber Service Module or CSM. One CSM per chamber is foreseen. It accepts up to 18 FE-links and sends the received data to a ROD far end board via a S-link type fiber. The CSM will synchronize all FE links onto a single fiber;

the ROD far end board, called Tower Service Crate (TSC), is a tower assembly module which can accept up to 6 input links, a number sufficient to build up a trigger tower as suited for Level-2 trigger calculations. Assembled data are sent via S-link from the ROD to a ROB.

A block diagram of the readout components is shown in Figure 15. A detailed description of the MDT readout options versus link occupancy is reported in reference *[14]*.

The choice of which CSM fibers to attach to each TSC determines the data pattern within the ROB memories and hence strongly affects the location of the trigger data needed by Level-2. The connection arrangement also determines the data rate from the TSC to the ROB.

Among many possible options for the readout segmentation, a choice of approximate rapidity towers is made, where a tower is built within a ROB (barrel) or within a crate of ROBs (endcap). By taking η towers in the barrel or ϕ towers (subsequently arranged in η towers) in the endcaps, data flow and trigger requirements are compatible since the data flow can be averaged over high and low rate chambers. This is better described in the next subsections.

6.2.1 Barrel

In the barrel the ϕ segmentation is 16-fold, where *large* and *small* chambers alternate. In the z direction there are 12 chambers ($|\eta| < 1$), built with approximate projective tower geometry. In each station two longitudinally adjacent chambers are grouped together in the readout in order to form 6 segments in z, 3 for each half barrel (negative and positive η). They will form an equivalent number of trigger towers from the three MDT stations BI, BM and BO as reported in table 24. Data from each tower are routed into a single ROD.

This barrel segmentation and channel grouping exploits data locality in the ROBs versus Level-2 trigger requirements. According to the Level-2 trigger algorithm, given the size of the largest road in the MDTs, data will be always found in a few ROBs (two or three at most). It is worthwhile to remember that this readout grouping option is based on the fact that the bending plane of the muons in the toroidal field is the r-z plane.

An alternative scheme, where a *large* and a *small* chamber adjacent in ϕ are grouped together, will be evaluated later. This scheme would give a more balanced data rate in the trigger towers but would increase the number of ROB fragments to be collected by the Level-2 trigger. If acceptable from the point of view of the trigger data flow, this option can be considered at a later stage and easily implemented with the present ROD design.

The arrangement of data from MDT towers into RODs is shown in figure 16. In the same figure is shown the ROD/ROB mapping. Two possible options are indicated : one foresees crates with 6 ROBs with data from large or small chambers only, covering one octant of the full barrel; the other option foresees crates with 6 ROBs, 3 for large chambers and 3 for small chambers, covering one octant of half barrel (negative or positive η). The picture of the entire data flow, from a given η–ϕ region of the detector, will be completed by the description of the trigger chambers which map the precision ones.

6.2.2 Endcap

In the endcap region a 16-fold ϕ segmentation is adopted. Two different readout schemes can be envisaged : one forming ϕ groups of chambers for each sector in each station and building up η-towers at the ROB crate level; the other forming directly η-towers at ROB level by summing data from the different stations, at a fixed η interval. The favourite option

for cabling reasons and also for the Level-2 algorithm, seems to be the first one. Data belonging to a η tower will be found in the same crate. We remind that in the endcap region, differently from the barrel, muons are also bended in the r-ϕ plane.

The arrangement of data from MDT towers into RODs is shown in figure 17. In the same figure it is shown the ROD/ROB mapping and the arrangement of ROB crates. They will contain 3 ROBs for large chambers and 3 ROBs for small chambers, covering one full octant of one endcap. The alternative option of η towers at the ROB level will be evaluated at a second stage. Presently we know that it is compatible with link occupancy. A summary of readout options based on ϕ-groups of chambers is reported in table 24.

The picture of the entire data flow from a given η–ϕ region of the detector will be completed by the description of the trigger chambers which map the precision ones.

6.2.3 Summary

The readout choosen as first option for both barrel and endcaps gives the number of ROBs reported in table 24. Therefore the barrel RODs form projective towers, but the endcap RODs do not.

MDT readout segmentation into a single ROD.		**Δϕ large/small**	**|η|**	**# channels large/ small**	**#RODs** (x2 for +-η)
Barrel Group 1	*(BIL+BML+BOL 1&2)* *(BIS+BMS+BOS 1&2)*	*0.52* *0.26*	*0.0-0.46* *0.0-0.40*	*2112* *2016*	***16x2***
Barrel Group 2	*(BIL+BML+BOL 3&4)* *(BIS+BMS+BOS 3&4)*	*“*	*0.46-0.86* *0.40-0.75*	*1872* *1968*	***16x2***
Barrel Group 3	*(BIL+BML+BOL 5&6)* *(BIS+BMS+BOS 5&6)*	*“*	*0.86-1.07* *0.75-1.03*	*1872* *1776*	***16x2***
Endcap Group 4	*EIL(1&2&3&4)+EEL(1&2)* *EIS(1&2)+EES(1&2)+BIS(7+8)*	*“*	*1.07-2.03* *1.03-1.93*	*1632* *1536*	***16x2***
Endcap Group 5	*EML(1&2&3&4&5)* *EMS(1&2&3&4&5)*	*“*	*1.07-2.70* *1.03-2.71*	*1872* *1920*	***16x2***
Endcap Group 6	*EOL(1&2&3&4&5&6)* *EOS(1&2&3&4&5&6)*	*“*	*1.36-2.70* *1.36-2.71*	*1824* *1872*	***16x2***
Total				***36 x 10^4***	**192**

Table 24: Readout segmentation of MDT tubes into RODs. Remember, the endcap RODs do not form projective towers, but overlap as layers.

6.3 Occupancy

Link occupancy has been calculated with a simulation program based on the following assumptions:

average tube length used for chambers with changing dimensions;

maximum rate used for a given chamber module;

hit rates from the setup named TP43;

safety factor of 5 included;

minimal overhead of headers and trailers in the data;

one FE-link per TDC, 1 Hot-link (or S-link type) per CSM (as output), at most 6 Hot-links per TSC in input and 1 S-link per TSC in output.

The maximum required bandwidths per link are :

FE-link (2 meters long) : 40 Mbits/s;

CSM-link (80-100 meters long) : 40 MBytes/s;

S-link (short) :0.66 Gbits/s.

Results on link occupancy in % are not presented as such, instead the total data rate into each ROB is calculated separately. These numbers are presented in table 25 for barrel and endcaps. More details can be found in *[14]*.

6.4 Data into ROD

The documents *[15]* and *[16]* describe the detailed formats delivered by the readout components. These formats are preliminary and subject to change while the ROD design evolves.

Each TDC sends data over one FE-link but the option to group many TDCs on one link is retained and delimiters for TDC groups may appear in the data format. By default, one group contains only one TDC. The TDC data blocklet foresees a header and a trailer as delimiters.

6.5 Data from ROD to ROB

The data format from ROD to ROB will follow the specifications described in *[17]*.The far-end ROD, the TSC, will insert headers and trailers in the data flow, including identifiers specially defined for the muon system.

The event format from ROD to ROB will look as follows:

ROD Header	32 bits
Data elements (with status)	see below for bits
ROD trailer	32 bits

where each data elements will be organized as follows:

Group Header	32 bits
TDC data	see below for bits
....	....
TDC data	....
Group Trailer	32 bits

and each TDC data will be

TDC Header	32 bits
Data	32 bits
...	....
Data	....
TDC Trailer	32 bits

The total data volume which is expected between RODs and ROBs has been estimated using the simple simulation program described earlier. The detailed numbers relevant to each ROB are given in table 25. The rates vary from **2 to 6 kbits/ROB/event**, assuming a 75 kHz LVL1 trigger rate.

6.6 Data from ROB to FEX

The muon FEX algorithm will require data belonging to a precalculated road in the MDT to perform the pattern recognition of the muon track. From the computed road sizes, data corresponding to a RoI will consist of a few ROB fragments (say 3-4). One ROB contains data from two longitudinal adjacent chambers, therefore a region much larger than the RoI size as defined by LVL1. It is planned to transfer the full content of a ROB to the FEX algorithm which will search for the hits in the road among the available data.

No special format or data reduction is foreseen at the ROB level. Data decoding will be the first step of the algorithm, after data collection. The pattern recognition will be performed at the 'tube' level followed by the use of the drift time information applied only to the hits which survive this step.

MDT readout group		ROB Data rate (kbits/event)	ROB Data rate (Gbits/sec)
Barrel Group 1	*(BIL+BML+BOL 1&2)* *(BIS+BMS+BOS 1&2)*	*3.9* *3.2*	*0.29* *0.24*
Barrel Group 2	*(BIL+BML+BOL 3&4)* *(BIS+BMS+BOS 3&4)*	*6.9* *4.7*	*0.52* *0.35*
Barrel Group 3	*(BIL+BML+BOL 5&6)* *(BIS+BMS+BOS 5&6)*	*3.9* *2.7*	*0.29* *0.20*
Endcap Group 4	*EIL(1&2&3&4)+EEL(1&2)* *EIS(1&2&3&4)+EES(1&2)+BIS(7)*	*8.8* *8.8*	*0.66* *0.66*
Endcap Group 5	*EML(1&2&3&4&5)* *EMS(1&2&3&4&5)*	*8.4* *8.4*	*0.63* *0.63*
Endcap Group 6	*EOL(1&2&3&4&5&6)* *EOS(1&2&3&4&5&6)*	*4.3* *4.1*	*0.32* *0.31*
Total			

Table 25: Summary of MDT data rates into ROBs, assuming a 75 kHz LVL1 trigger rate.

Presently it is not foreseen to use CSC data in the Level-2 algorithm.

Figure 11: 3-D view of Muon Spectrometer instrumentation

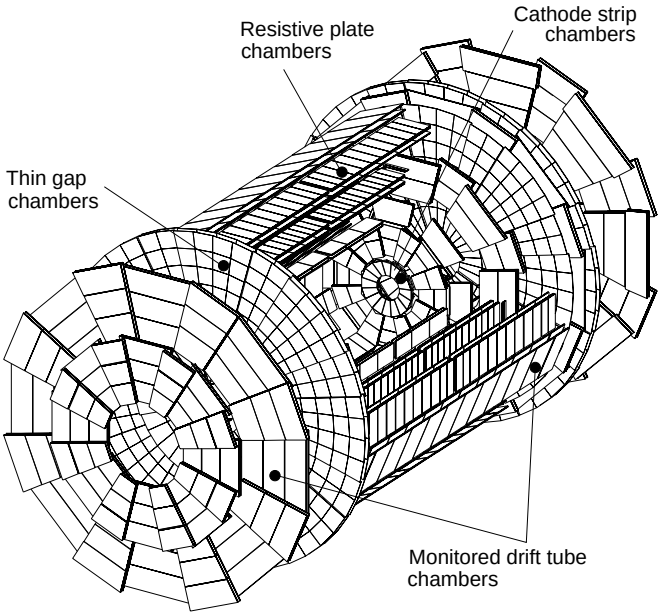

Figure 12: Side view of half spectrometer and definition of pseudo-rapidity towers

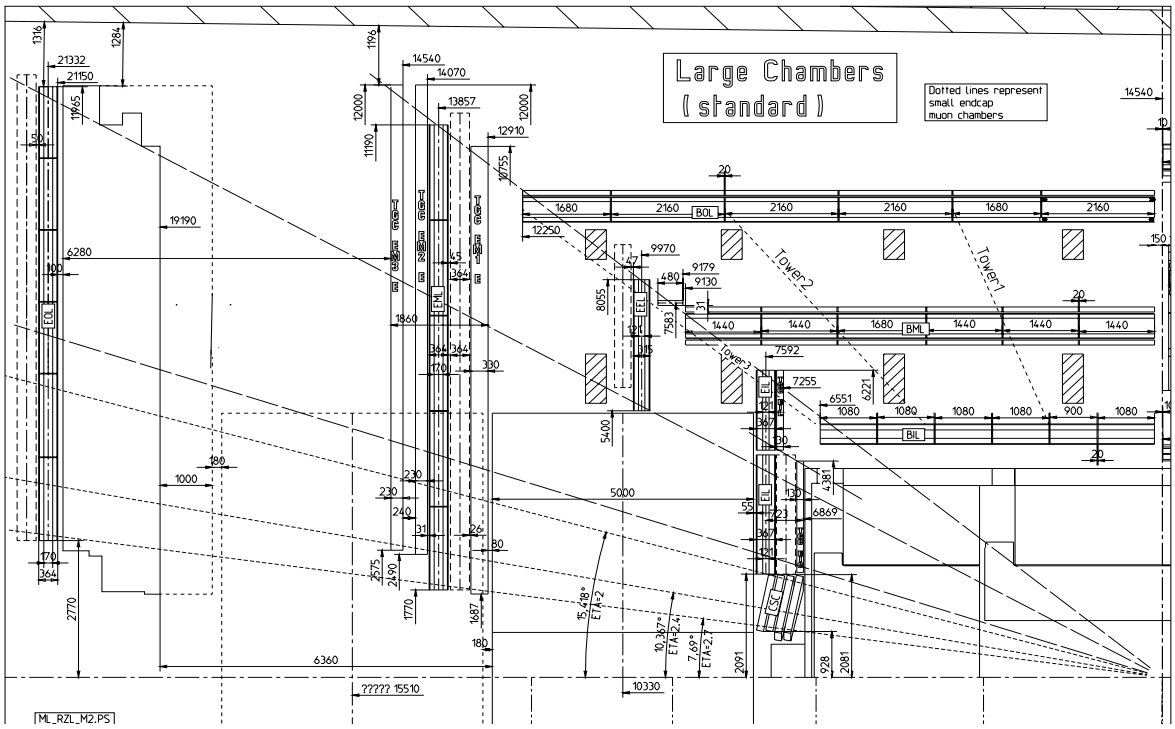

Figure 13: Transverse view of the barrel chambers and definition of sectors

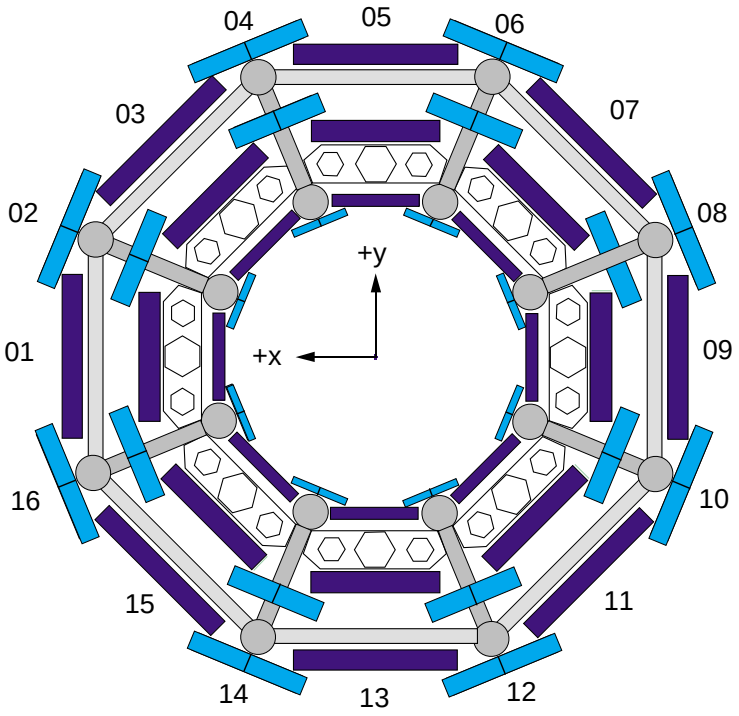

Figure 14: Arrangement of tubes in the MDT chamber and numbering convention for tubes connected to a TDC

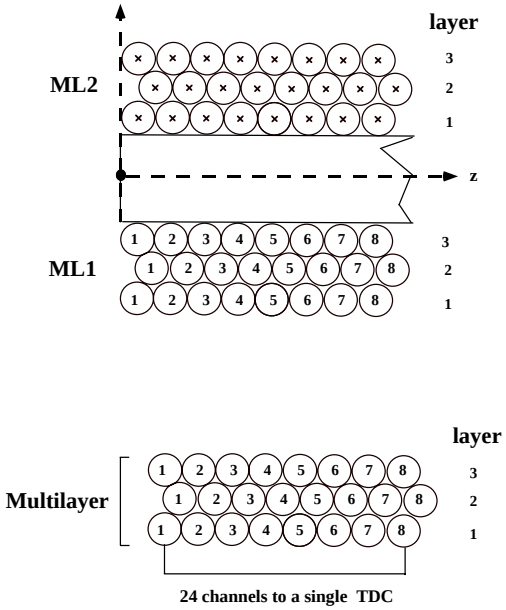

Figure 15: MDT readout chain, from Front-End to ROD

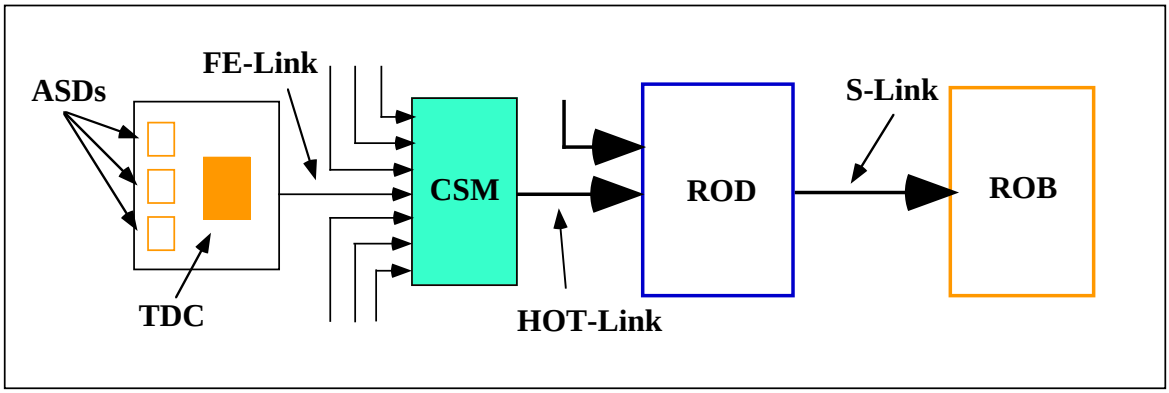

Figure 16: Barrel MDTs: chamber readout into RODs and ROD/ROB mapping (ROB crates)

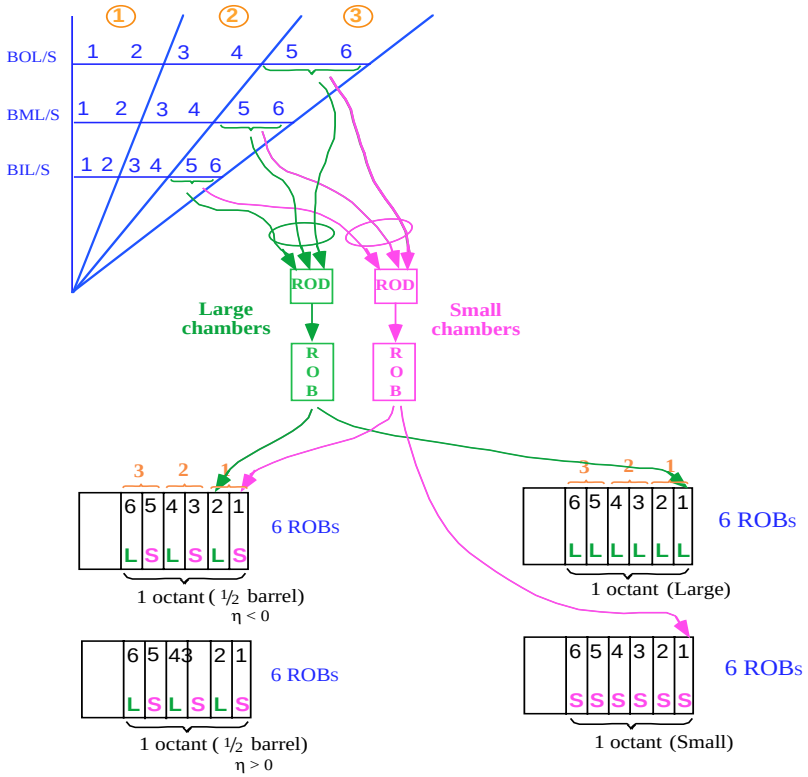

Figure 17: Endcap MDTs: chamber readout into RODs and ROD/ROB mapping (ROB crates)

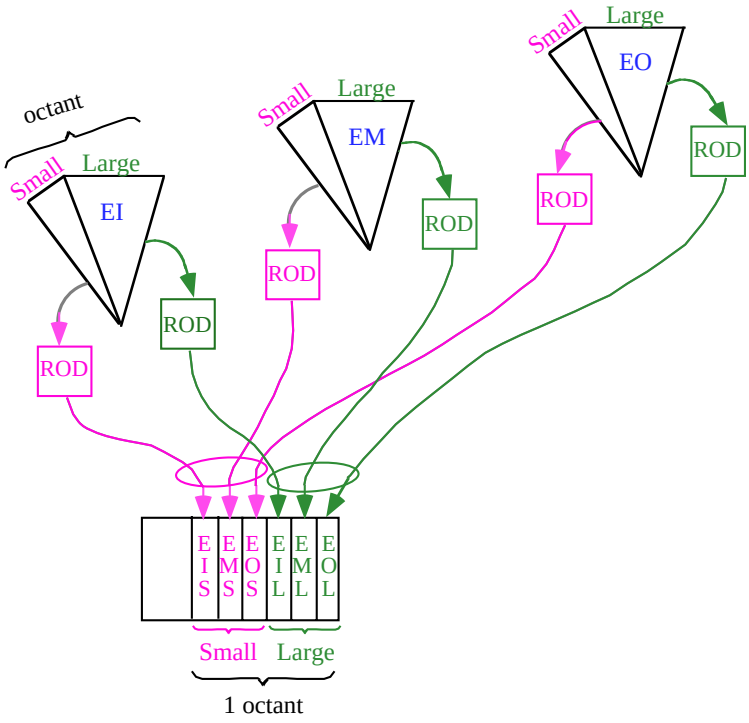

7 Muon Trigger Chambers

7.1 Geometry

The Level-1 muon trigger makes use of dedicated detectors, RPCs in the barrel region and TGCs in the endcaps. Details of the RPCs and TGCs can be found in *[13]* and *[18]*. An overview of the trigger chamber arrangement and the trigger system for the barrel and the endcaps is shown in figure 18.

Figure 18: Longitudinal view of the Level-1 trigger system and arrangements of trigger chambers in the spectrometer.

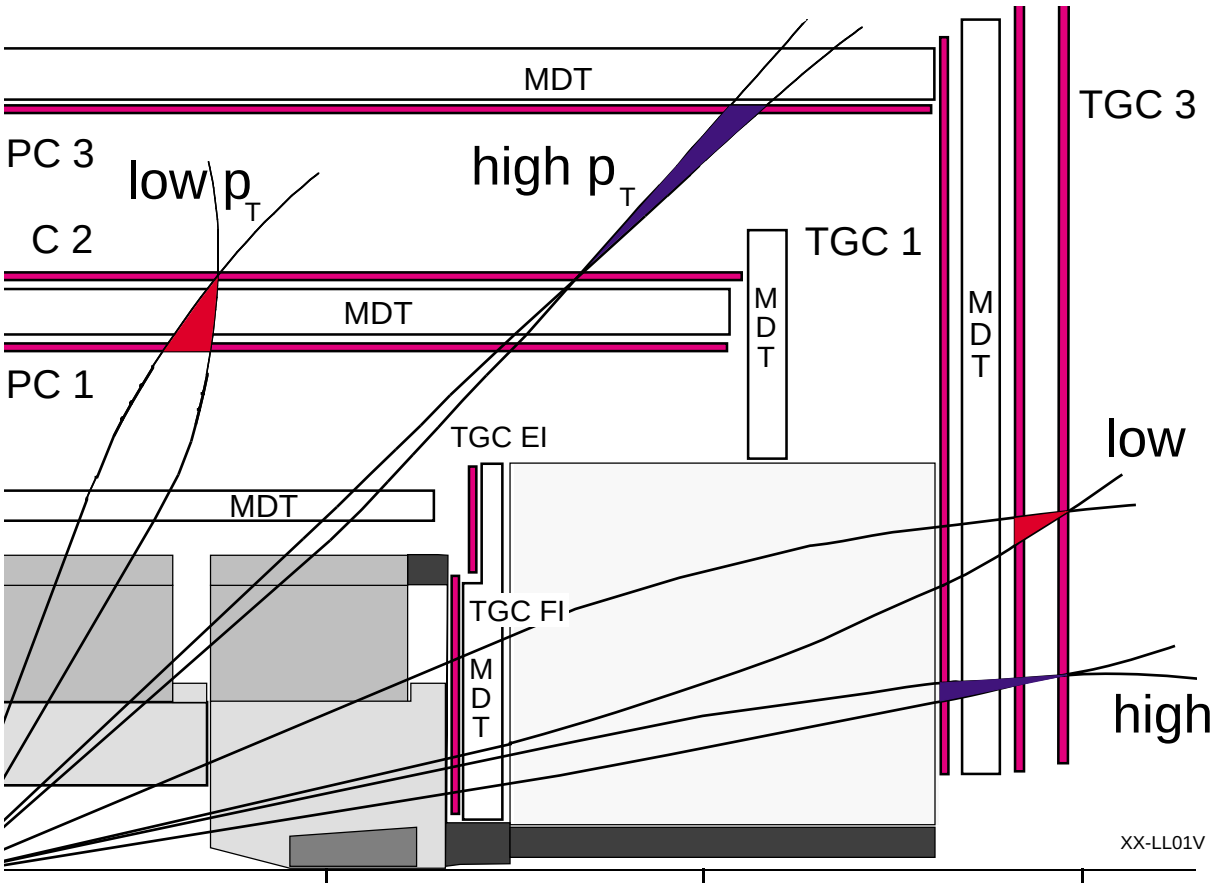

7.1.1 Barrel

The RPCs are used in the barrel region $\eta<1.03$. The trigger detector is organized in three stations, two of which are located above and below the MDT chambers in the middle station (RPC1 and RPC2), and the third one in the outer station (RPC3).

Each RPC station consists of two planes of readout strips: one in the transverse and one in the longitudinal direction. Both planes are used in the trigger. The η–strips are parallel to the MDT wires (bending view of the trigger detector). The ϕ-strips are orthogonal to the MDT wires and provide the second coordinate measurement.

Approximately 600 RPC chambers will be used in the spectrometer. Their dimensions have been choosen to match those of the corresponding MDTs but with higher granularity.

Table 26 summarizes some of the parameters of the RPC chambers for the layout M.4.

Nb. of chambers	*596*
Total nb. of longitudina channels	*235176*
Total nb. of transverse channels	*120496*
Total nb. of channels	*355672*

Table 26: Summary of RPC parameters.

7.1.2 Endcap

TGC trigger chambers are arranged in the detector in seven layers in each endcap at $|z| \sim 14$ m. They are grouped in three planes in z, one plane of triplet units and two planes of doublet units. The pair of doublets are the farthest planes from the interaction point in both endcaps, while the triplet is the nearest one. The triplet and the doublets are separated by the endcap MDT chambers of the middle station (EM). For triggering, the TGCs cover the pseudorapidity range $1.03 < |\eta| < 2.4$. Each TGC plane consists of a 'wheel' of eight octants of chambers symmetric in ϕ. The 'wheel' is divided in two rings, *Endcap* and *Forward* (see Fig. 1). The division between them is projective back to the interaction point. Wire groups give the η coordinate and strips the ϕ. The number of wires in a group varies according to the magnetic field strength.

Table 27 summarizes some of the parameters of the TGC chambers for the layout M.4.

Nb. of doublets plus triplets	*1584*
Nb. of wire channels	*220448*
Nb. of strip channels	*101376*
Total nb. of channels	*321824*

Table 27: Summary of TGC parameters.

7.2 Readout segmentation

7.2.1 Barrel

The Level-1 muon trigger logic and its segmentation is strongly coupled to the RPC chamber layout. The *large* and the *small* chambers of both middle and outer RPC stations, are logically divided in two to produce *two large* sectors and *two small* sectors per half-barrel octant.

From the trigger point of view, the barrel is divided in two parts (positive and negative η) and for each part 32 ϕ trigger sectors are defined. Therefore the system is logically segmented into 64 identical sectors.

Inside a sector, the trigger is segmented in PADs and ROIs (see definition later). The PAD segmentation is different for *large* and *small* sectors, following the chamber layout. A *large* sector contains 6 PADs while a *small* sector contains 7 PADs. The sector segmentation is shown in figure 19.

Figure 19: Barrel trigger segmentation. Areas covered by η and ϕ CMs, PADs and RoIs, are also indicated.

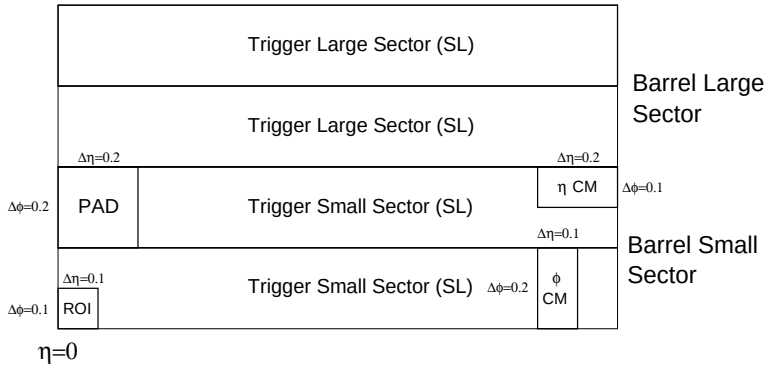

The signals from the RPCs are amplified, discriminated and digitally shaped on the detector. The Amplifier-Shaper-Discriminator (ASD) boards, each containing eight ASD channels, are placed on the chambers on one strip end.

In the *low-p_T* trigger, for each of the η and ϕ projections, the RPC signals of the two detector doublets, RPC1 and RPC2, are sent to a Coincidence-Matrix (CM) contained in a CM chip. This chip performs almost all the functions needed for the trigger algorithm and also for the readout of the RPC strips. It aligns the timing of the input signals, performs the coincidence and majority operations, and makes the p_T cut on three different thresholds. It also contains the Level-1 latency pipeline memory and derandomizing buffer.

The *high-p_T* trigger uses the results of the *low-p_T* trigger and the information generated by the RPCs in the outer station (RPC3). Those inputs are sent to a CM which applies an algorithm similar to that of the *low-p_T* trigger.

Four CMs are needed for the full trigger logic : two for the *low-p_T* trigger and two for the *high-p_T* trigger; each logic needs two CMs to handle the strips in the ϕ and η projections.

The information of two adjacent CMs in each of the two projections are combined together in a Pad Logic board (PAD). From the PAD, the combined information is sent synchronously at 40 MHz to the Sector Logic (SL) board, for trigger purposes, and to the ROD, for the readout.

The RPC and the barrel Level-1 muon trigger readout is schematically illustrated in figure 20.

Figure 20: RPC and Level-1 muon trigger readout chain.

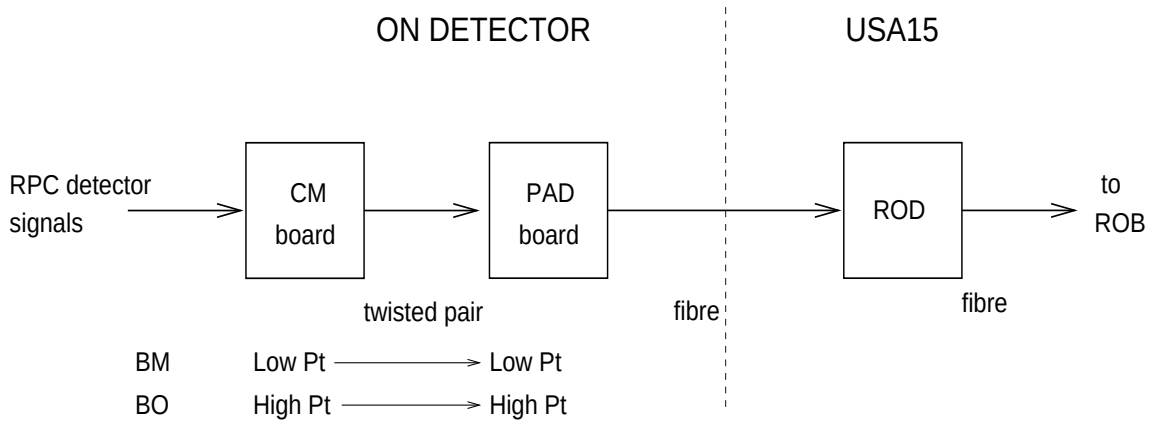

The RPCs and the Sector Logic of the Level-1 muon trigger are read out by 16 RODs for each half barrel, 32 RODs in total. The ROD collects the information, of both middle and outer chambers, of two *large* or two *small* sectors. In the *large* sectors the number of PADs connected to the ROD is 6 x 4 CMs x 2 sectors = 48. In the *small* sectors the number of PADs is 7 x 4 CMs x 2 sectors = 56. The connection from the PADs to the ROD is implemented through a 20 Mbit/s copper serial link. The ROD receives data from 24 (or 28) links, does the formatting, and sends data to the ROB via S-link.

The numbers of the readout components for the barrel trigger chambers are reported in table 28.

It is worthwhile to mention that, in order to make the trigger more robust, the trigger algorithm has been exended with additional programmable options. The options, presently under investigation, make use of the third trigger station also for the *low-*p_T trigger and of the tile calorimeter to require additional coincidences for the muon candidates. The readout scheme of the tile calorimeter has not yet worked out.

Nb. of FE and Trigger links	*416*
FE links receiver boards	*128*
Nb. of RODs/ROLs/ROBs (half barrel)	*16*
Nb. of RODs/ROLs/ROBs (full barrel)	*32*

Table 28: RPC readout parameters.

7.2.2 Endcap

The trigger algorithm extrapolates pivot plane (TGC3) hits to the interaction point to reconstruct the infinite-momentum path of the track. The deviation from this path in the preceding trigger planes is related to the track momentum.

The signals generated by the TGC chambers are amplified, discriminated and shaped by the on-detector "ASD" electronics. Signals from ASD boards are sent to a Patch Panel board which routes the signals from several layers of chambers to a 32-channel wide coincidence unit, called a "Slave Board". Bunch-crossing identification is done on the Patch Panel before the coincidence unit. The Slave Board also provides the readout of the chamber hits. There are four types of Slave Boards: wire and strip boards for each of the triplet and doublet-pair. They differ in the number of inputs, the type of coincidence made and the maximum window width.

Information from the Slave Boards is encoded to produce more compact signals to be sent to the *high-*p_T trigger coincidence Board. Here, signals from the doublet-pair and triplet Slave Boards are combined to check if they satisfy the *high-*p_T conditions. Wire (r-coordinate) and strip (ϕ-coordinate) are treated separately.

Signals from the *high-*p_T Boards are sent to the Sector Logic Boards containing an r-ϕ coincidence unit and track selectors, to select the highest p_T coincidences.

Detector and trigger data are readout in parallel. The readout is via a two level hierarchy. Data links from several Slave Boards of one or more trigger sectors, called a Local DAQ Block (LDB), are concentrated in a Star Switch. The switch is then connected via a fiber optic link to the ROD crate.

The main readout components (see figure 21) are:

Slave Board: contains the Level-1 pipeline, a derandomizer and a slave link interface. Up to 128 signals are handled by one Slave Board.

Star Switch: is a multiplexor with readout sequence logic. It has up to 32 input slave link interface connections and one optical link to a Local DAQ Master in the ROD crate.

Local DAQ Master: is an intelligent FPGA-based IO controller in the ROD crate that builds events from fragments and stores them in a buffer memory read out by the ROD.

ROD: manages the event fragment assembly, event formatting, accumulation of diagnostics, reporting of errors, and transmission to the ROB. The numbers of the readout components for the endcap trigger chambers are reported in table 29.

	One octant	**One endcap**	**Total**
Readout Slave boards	*234*		*3744*
Star Switches	*15*		*240*
Local DAQ Masters	*15*		*240*
Nb. of RODs/ROLs/ ROBs	*1*	*8*	*16*

Table 29: TGC readout parameters.

The Level-1 endcap trigger provides ROIs defined as cells in the r-ϕ space in which a muon track candidate has been found, crossing at least one of the six configured thresholds. For triggering purposes, the octants of the pivot plane (TGC3) are divided in two regions, *endcap* (η < 1.9) and *forward* (η > $ 1.9). Each *endcap* octant is divided into six trigger sectors in ϕ, where a trigger sector is a logical unit treated independently by the trigger system. Similarly, each *forward* octant is divided into three trigger sectors. Trigger sectors are further divided into η–ϕ trigger subsectors, each corresponding to a ROI. Subsectors are 8 channels by 8 channels. Since the wire groups are not of constant size in η, the ROI extent in η is also not regular. Typically ROIs are about .03 by .025 in η–ϕ. The trigger segmentation of an octant is shown in figure 22.

Figure 21: Implementation of endcap muon trigger chamber readout for an octant.

Muon Endcap trigger chambers (TGC) readout for 1 of 16 octants

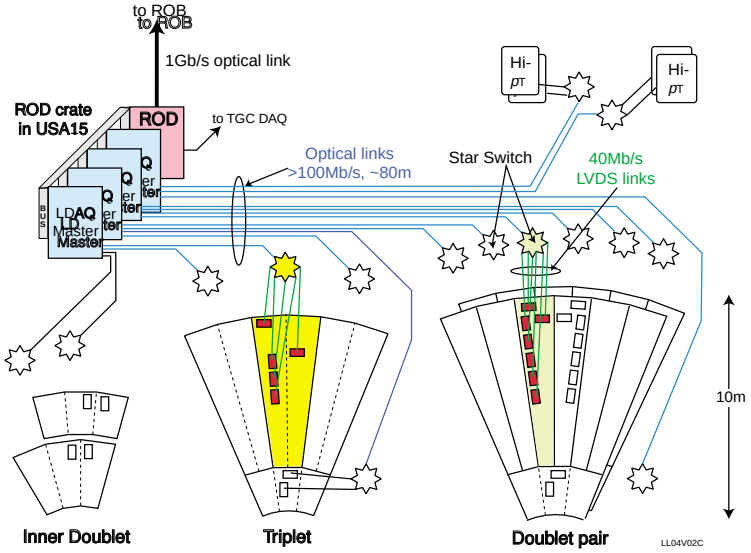

Figure 22: TGC Level-1 trigger segmentation for one octant.

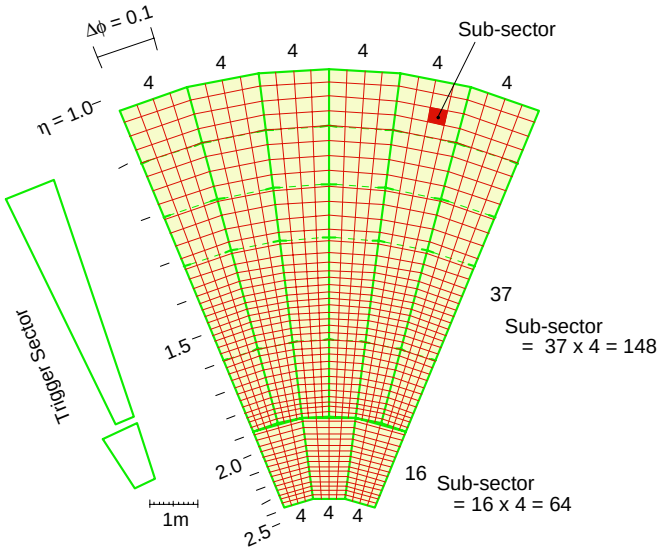

7.3 Data into the ROD

7.3.1 Barrel

The ROD functionality includes:

data collection from Front-End links;

data integrity checks;

Front-End link to Readout Link (ROL) format conversion;

handling of busy signals;

error detection and recovery.

	Identifier	**Nb. of bits**
Absolute ROD number	*0-31*	*5bit*
Absolute SL number	*0-6*	*6 bit*
PAD number within SL	*0-7*	*3 bit*
CM number within PAD	*0-3*	*2 bit*

Table 30: RPC readout identifiers and numbering.

For a *low-p_T* muon candidate, a CM generates on average 16 bytes (four clusters from the RPC1 and RPC2 doublets). An additional 10 bytes have to be accounted for a *high-p_T* trigger. Each trigger produces 4 bytes in output (2 bytes for the hit patterns and two bytes for the thresholds/overlap information).

Each RPC hit strip will be encoded in 2 bytes including strip number and time-interpolator measurement as shown in figure 23.

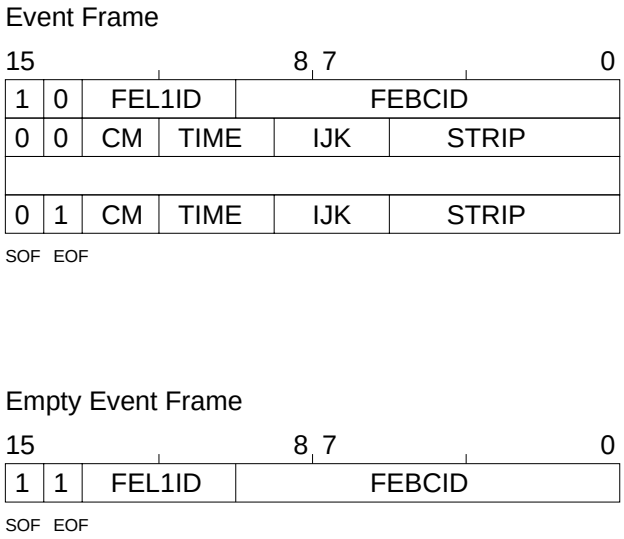

Figure 23: CM to PAD and copper link data format.

Some additional information such as Front-end BCID, Front-end L1ID, is inserted along the data flow for synchronization checks. Sector Logics will also send readout data to a dedicated SL ROD for monitoring purposes.

Table 31 shows the average required bandwidth from CM to ROD with and without data encoding.

	Link bandwidth	**Average bandwidth (16 bit encoding+headers)**	**Average bandwidth (no encoding)**
CM to ROD	*10 Mbit/s*	*1.5 Mbit/s*	*240 Mbit/s*
ROD to ROB	*1 Gbit/s*	*0.36 Mbit/s*	*50 Gbit/s*

Table 31: RPC chambers : average required bandwidths.

7.3.2 Endcap

Table 32 shows the average required bandwidths along the endcap readout data flow.

Station total		*No. LDBs*	*Slave Boards*	*No. Channels*	*Raw MB/s*	*Hit/ event*	*Encoded KB/s*	*Overhead KB/s*
Doublet *64* *1331*	*F* *E*	*1* *6*	*15* *90*	*1902* *11124*	*23.8* *139.1*	*0.11* *2.22*	*32.0* *665.3*	*32.0* *665.3*
Triplet *41* *341*	*F* *E*	*1* *3*	*15* *54*	*1200* *5172*	*15.0* *64.7*	*0.07* *0.57*	*20.4* *170.7*	*20.4* *170.7*
Inner *120* *76*	*F* *E*	*1* *1*	*3* *3*	*380* *336*	*4.8* *4.2*	*0.20* *0.13*	*59.8* *38.1*	*59.8* *38.1*
One octant *1972* *two sides* *31559*		*15* *240*	*180* *2880*	*20114* *321824*	*251.4* *4022.8*	*3.29* *52.60*	*986.2* *15779.6*	*986.2* *15779.6*

Table 32: Estimated data flow for 1 of 16 TGC octants. Rates are for 100 KHz Level-1 rate. Hits are dominated by uncorrelated background, based on TP32, plus electronic noise.

7.4 Data from ROD to ROB

7.4.1 Barrel

ROD data, when sent to the ROB, will be formatted according to the standard DAQ format described in *[17]*.

The RPC data format from ROD to ROB is reported in figure 24.

Figure 24: RPC ROD data format.

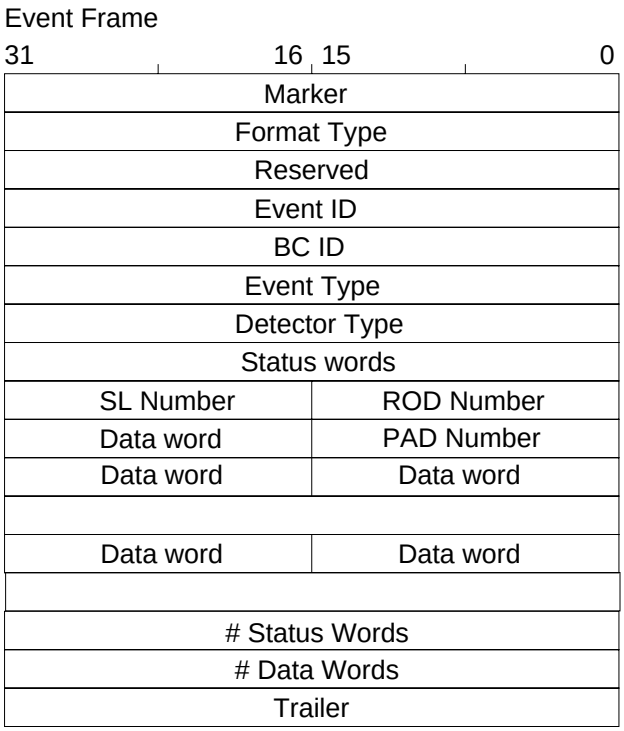

7.4.2 Endcap

The format of a TGC hit sent to the ROB is shown in table 33.

This format is in terms of chamber objects and is more suited to track finding than the data-path format used inside the ROD. The wire-groups are numbered across chamber boundaries within a sector.

There is one ROB per octant so that a TGC ROB for an octant can sit in the same ROB crate as the MDT ROBs for that octant. The radial boundary between large and small MDT chambers roughly corresponds to a TGC sector boundary. The TGC hits are ordered in the ROB by sectors in such a way that the hits from sectors corresponding to an MDT chamber follow each other.

endcap	*octant*	*sector*	*w/s*	*layer*	*logical chan*

Table 33: The format of a TGC hit sent to the ROB

7.5 Data from ROB to FEX

The Level-2 muon algorithms, barrel and endcap, make use of trigger chamber data to guide the pattern recognition in the precision chambers, the MDTs. Therefore RPC and TGC data belonging to the muon RoIs will be sent to the FEX and used to calculate a first approximation muon trajectory.

A possible readout option for the muon chambers is based on the assumption that RPC and MDT data from the same projective area are found in ROBs sitting in the same DAQ crate. This would allow for local pre-processing which needs data from both detectors. For example the splitting of the present trigger algorithms in two stages performed before and after the Level-2 switching network, can place the selection of the MDT hits belonging to the muon road at the ROB crate level or in the RSI if RPC and MDT ROBs are not mixed.

In this scheme, only MDT data would be sent from the ROB to the FEX thus reducing the data volume through the switch (the amount of the reduction and the feasibility of this option have still to be calculated).

8 Muon to CTP Interface (MUCTPI)

The MUCTPI receives muon candidates from the Sector-Logic of the muon trigger chambers (RPCs in the barrel region and TGCs in the Endcap and Forward regions.) In the MUCTPI three tasks are executed:

- Muon candidate multiplicities for the whole muon trigger chamber system are formed at six different pt-thresholds. These multiplicities are sent to the Central Trigger Processor (CTP) which forms the LVL1 trigger decision.
- For every event accepted by LVL1 (LVL1A), muon candidates are sent to the ROI-Builder of the LVL2 system.
- For every LVL1A, muon candidates and the formed muon multiplicities are sent via a ROD into a ROB.

A detailed description of the system can be found in *[18]*. Details of the data sent to the LVL2 system are summarised in *[19]*.

8.1 Structure of the MUCTPI

The MUCTPI is housed in one crate containing three different modules. Figure 25 shows

Figure 25: Block diagram of the MUCTPI

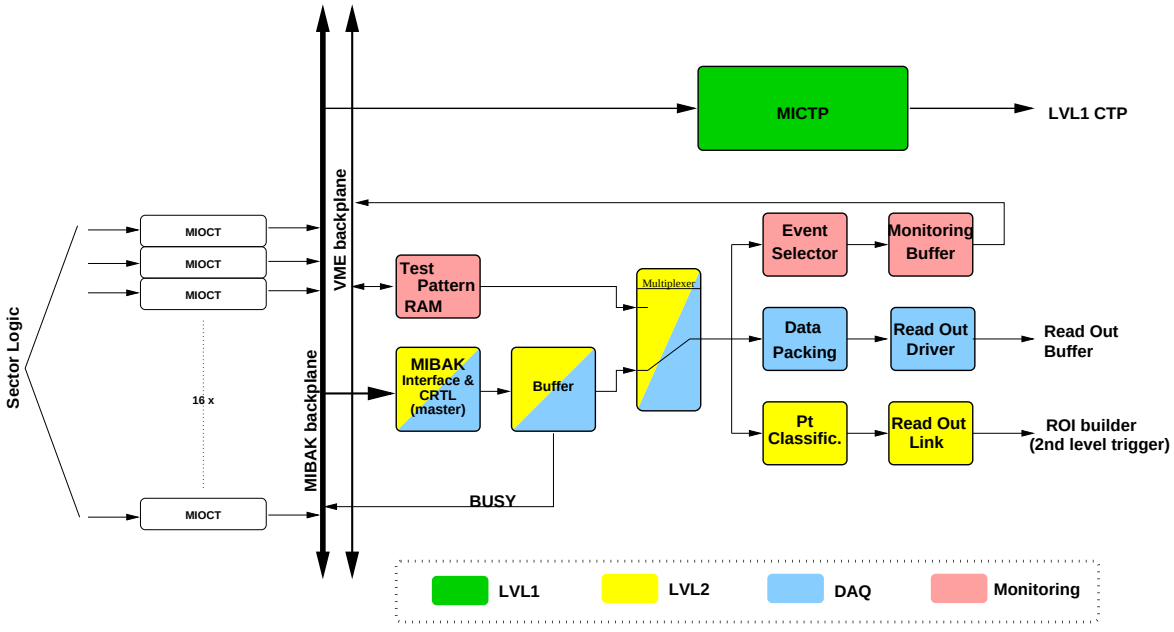

the blockdiagram of the MUCTPI. Units relevant for data transfer to the DAQ system and to LVL2 are shown more detailed. Muon candidates are received from the Sector Logic by 16 octant boards (MIOCT). Together with the active backplane MIBAK they form the multiplicities for LVL1, which are sent via the MICTP module to the CTP. On a LVL1A they send zero-suppressed candidates to the MIROD module which is shown more detailed. It contains the interface to the ROI-Builder and the ROD.

8.2 Readout segmentation

The segmentation of the muon trigger chambers has been described in detail in sections 7.2.1 and 7.2.2. Figure 26 summarizes this segmentation for one azimuthal octant. The

Figure 26: Segmentation of the muon trigger system

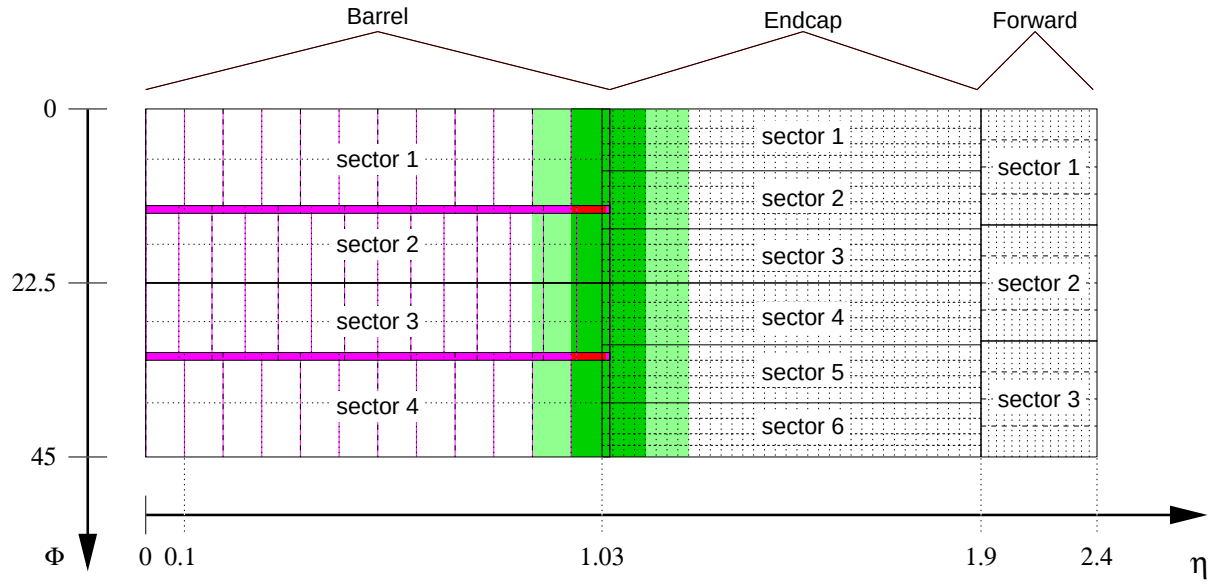

entire muon trigger system is formed by 16 such structures, eight for the the positive and eight for the negative rapidity regions. In the barrel region a sector contains 24 or 28 subsectors depending on whether it is built from large or small RPC-chambers. In the endcap 144, and in the forward region 60 subsectors are contained in a sector. The shaded regions indicate zones in which single muons can cause more than one candidate due to overlap of several trigger chambers.

8.3 Occupancy

The number of muon candidates which have to be transfered to the ROD and the ROB can be deduced from extensive studies on muon-trigger and background rates (see for example *[20][21][22]*).

At low luminosity the rate of muon candidates at low pt-threshold (6 GeV) is expected to be 25.2 kHz. (This number includes background rates and fake muon rates. It assumes the so called “full system” trigger scheme). This means that at a LVL1 trigger rate of 40 kHz 0.63 muon candidates per triggered event are expected.

At high luminosity the trigger rate due to muon candidates is lower. To the total LVL1-trigger rate of 40 kHz muon candidates exceeding the high pt threshold (20 GeV) are expected to contribute with approximately 5 kHz, the dimuon trigger (requiring at least two muons of 6 GeV) with 3kHz, and one muon of at least 10 GeV together with an isolated electromagnetic cluster with 400Hz. The number of muon candidates in random Bunch Crossing (BC) and be estimated to be ten times the low-pt muon candidate rate at low luminosity. The

resulting 252 kHz rate is very small compared to the BC rate of 40 MHz and therefore these candidates can be neglected even in the case that five bunch BCs are read out for every LVL1A. The number of expected muon candidates results in 0.3 candidate per event.

8.4 Data into ROD

The MUCTPI receives for every BC a data word from each sector of the muon trigger system. The words contain up to two muon candidates for each of which the exceeded transverse momentum threshold, the ROI identification and some flags are encoded. In the MIOCT modules data is zero suppressed so that for each LVL1A only data words containing valid muon candidates are sent via to the ROD. The system can be programmed to send candidates in a window of at most +/- 2 BCs around the LVL1A.

For each event the following data is sent into the ROD:

The total multiplicities of the six different transverse momentum thresholds. This data is sent for each BC of the programmed window around the LVL1 trigger.

All muon candidates which were found in the programmed window around the LVL1 trigger (details see below)

For each muon candidate the following information is sent to the ROD:

An identification code which allows to decode the subsector of the muon candidate.

The highest pt-threshold which the candidate exceeded.

Flags indicating that the candidate was found in a region which overlaps with other sectors. For barrel candidates two flags are sent, one indicating overlap with a neighbouring barrel sector, the other with a neighbouring endcap sector. Endcap candidates can only overlap with barrel sectors and hence only one flag is sent. There is no overlap flag for candidates in the forward region.

A flag indicating if there have been more than 2 candidates in a sector. In this case the two highest pt candidates are transfered.

A flag indicating that there has been more than one candidate in an endcap or forward subsector, or more than one candidate in a barrel Pad.

The three least significant bits of the BC identification number (BCID). This number comes from the Sector Logic and is used in the ROD to select muon candidates for the ROIB.

8.5 Data from ROD to ROB

The data sent to the ROB is very similar to what is received by the ROD. The identification code of the muon candidates is translated in the ROD into a more physical address identifying the origin of the candidate in terms of detector type, hemisphere and sector number. With every candidate a flag is sent indicating if the candidate is passed to the ROIB[1].

1. Programmable thresholds in the ROIB interface can prevent muon candidates from being sent to the LVL2 trigger.

A preliminary proposal for the data fragment sent from the ROD to the ROB is shown in figure 27. It is compliant to the ATLAS readout format suggested in *[17]*. Given the low candidate rates estimated above, the data rate into the ROB is dominated by the header and trailer words of the readout format. For an event with 2 muon candidates and a readout of 5 BCs, 20 words or 640 bits have to be transfered to the ROB.

8.6 Data from ROB to FEX

Currently it is not foreseen to to use the MUCTPI data in the Level-2 algorithms. An evaluation of this possibility has still to be done.

Figure 27: Preliminary Data format sent from the MUCTPI-ROD to the ROB.

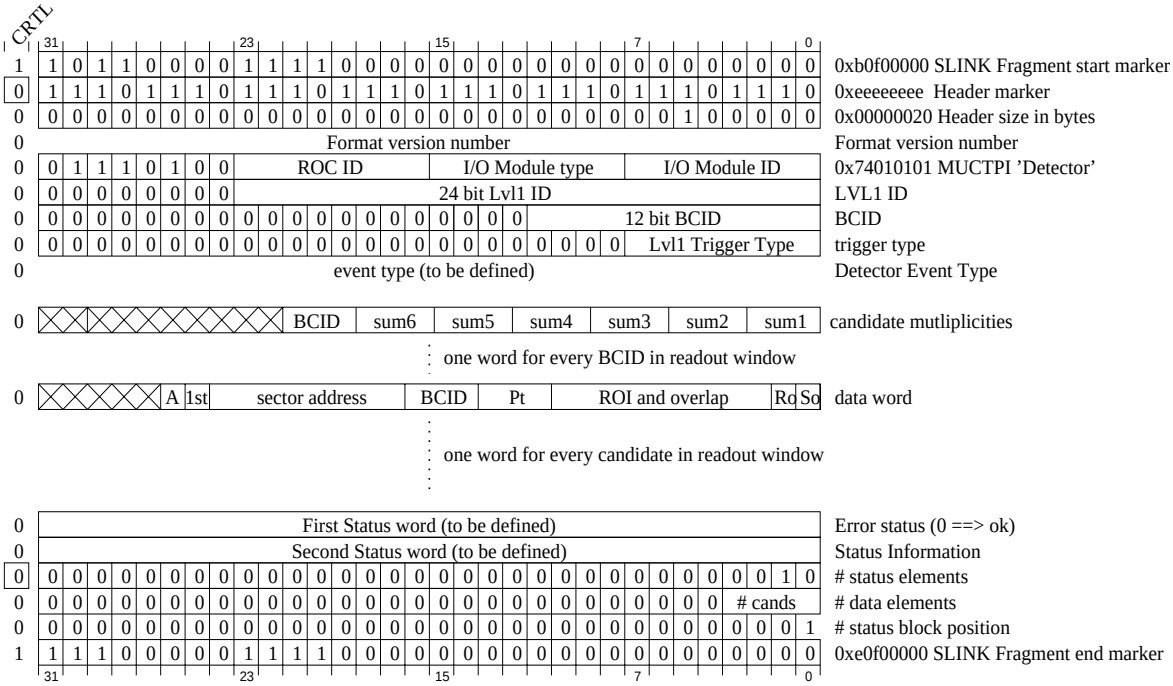

CRLT : SLINK control word flag
Pt : binary encoded Pt threshold (1 to 6)
1st : 1/0 most/second most energetic candidate in sector
Ro : more than 1 candidate in ROI
So : more than 2 candidates in sector
A : Candidate accepted and sent to ROIB
BCID : 3 bit BCID from Sector Logic
sumn : total candidate multiplicity for threshold n

9 Acknowledgements

The authors would like to express their sincere thanks to various people who supplied detailed information, and subsequently read over sections (any errors remaining are of course entirely the responsibility of the authors). Particular thanks go to: A.Lankford, P.Farthouat, R.Wastie, T.Jones, E.Anderssen, D.Fasching, R.Richter, L.Levinson and S.Veneziano.

10Bibliography

[1]ATLAS DAQ-Note-62.

[2]ATLAS Inner Detector Technical Design Report, ATLAS TDR-4&5, CERN/LHCC/97-16, 30-April-1997

[3]Philippe Farthouat, Private Comm.

[4]Matthias Sessler note on TRT algorithms, ATLAS DAQ-Note-98

[5]Sarah Wheeler, ATL-COM-DAQ-99-014, http://home.cern.ch/~wheeler/ROBresults.html ; Jos Vermeulen, http://www.nikhef.nl/pub/experiments/atlas/daq/modelling.html

[6]V.A.Charlton, ATLAS DAQ-Note-57, 10 Sept. 1996

[7]“SCT and Pixel Interfaces to the ROD” http://positron.ps.uci.edu/~rodatlas/abc_mcc.pdf

[8]ROD note “Readout Link Interface” http://positron.ps.uci.edu/~rodatlas/readout.pdf

[9]R.Dankers, PhD thesis, Universiteit Twente, 1998.

[10]ATLAS Pixel Technical Design Report, ATLAS TDR-11, CERN/LHCC/98-13.

[11]Damon Fasching, private communication, 6 June 1999.

[12]ROD demonstrator project; http://wwwnice.cern.ch/~efthymzp/rod/lardemorod_v2r2.doc

[13]ATLAS Muon Spectrometer Technical Design Report, CERN/LHCC/97-22, ATLAS TDR 10, 31 May 1997.

[14]Options for MDT Connections, J.Chapman and B.Ball, Nov. 1998 (Draft Report) http://umaxp1.physics.lsa.umich.edu/~chapman/atlas/CsmTrd.html, http://umaxp1.physics.lsa.umich.edu/~chapman/atlas/CsmTrd.ps, http://umaxp1.physics.lsa.umich.edu/~chapman/atlas/CsmTrd.pdf

[15]NIMROD, the ROD for the Monitored Drift Tubes in ATLAS, H.L.Groenstege et al., ETR 96-09, NIKHEF, Amsterdam, http://www.nikhef.nl/pub/departments/et/atlas_mdt/nimrod/

[16]AMT-0, ATLAS Muon TDC version 0, J.Christiansen, CERN/EP-MIC

[17]ATLAS DAQ-Note-98-129, D.Francis et al., http://atddoc.cern.ch/Atlas/Notes/050/Note050-1.html

[18]ATLAS First-Level Trigger Technical Design Report, CERN/LHCC/98-14, ATLAS TDR-12, 30 June 1998

[19]Specification of the LVL1 / LVL2 trigger interface, M.Abolins et al, ATLAS-DAQ-note in preparation, September 1999

[20]ATLAS Trigger Menu, J.Baines et al., ATLAS DAQ-NO-121, ATLAS PHYS-NO-124, 26-June-1998.

[21]ATLAS Trigger Performance Status Report, ATLAS / Trigger Performance Group, CERN/LHCC 98-15. 25 August 1998

[22]Improvements to the Level-1 muon trigger giving increased robustness against backgrounds, ATLAS Level-1 muon trigger gorup, ATL-DAQ-99-008, 23-July-1999.